Durham University
School of Engineering

Final Year Project

Structural Analysis of Geodesic Domes

Author:
Marek Kubik

Supervisor:
Charles Augarde

April 29, 2009

Abstract

A project to house 40 families in the Maharashtra region of India which began in January 2005 was halted shortly after it commenced due to concerns over the loading applied to a series of geodesic domes which form a large portion of the whole complex. Vigyan Ashram, the organisation that manufactures the domes, issued a request for the development of an affordable computer program that would allow them to model the structural response of the domes. The ensuing research into the design of the geodesic domes and the development of a spreadsheet based finite element package are the subject of this dissertation.

Acknowledgements

I wish to thank all at Vigyan Ashram, particularly Yogesh Kulkarni and Ashok Mathur, for their assistance with gathering information relevant to this project. I would also like to express my gratitude to Colin Wintrip and Steven Richardson, whose assistance with fabricating and testing the joints was greatly appreciated. Finally, I wish to thank Dr. Charles Augarde, my supervisor, who has provided me with invaluable guidance and advice throughout this research project.

Project plan

Introduction

A project to house 40 families in the Maharashtra region of India which began in January 2005 was halted shortly after it commenced due to concerns over the loading applied to a series of geodesic domes which form a large portion of the whole complex. The domes had soil packed over them, a condition which was never anticipated in the original design. The need for a method to model the structural response of the geodesic or "Pabal" dome was highlighted by Vigyan Ashram, the Non Governmental Organisation (NGO) that manufactures the domes; this dissertation describes the research into the Pabal dome and the development of a bespoke finite element analysis (FEA) package capable of running in Microsoft Excel.

Objectives

Vigyan Ashram locally produces the geodesic domes as do-it-yourself kits for the lower-middle class of both rural and urban populations. The original design was adopted in the aftermath of the 1993 Killari earthquake, aiming to provide durable, low cost housing capable of withstanding the earthquakes, rains and winds of India for those that lost their homes.

Of the 120 geodesic dome kits supplied to the Water Bank housing project, 40 were planned to be subterranean and were therefore affected. Vigyan Ashram, together with another NGO, engINdia, asked for research into the geodesic dome's current incarnation to be carried out. The Water Bank project highlighted the need for a method of modelling the structural response of geodesic domes, as an assessment of the loading encountered by the domes would allow recommendations to be made as to how the design could be adapted to accommodate the expected loading.

Vigyan Ashram's main desire was for a structural analysis package without the associated licensing costs, to allow their science and technology centre to assess the geodesic dome's structural response in-house. This would provide significant long term benefits for Vigyan Ashram, removing the need for outsider aid with such design problems in the future. If appropriate, students at Vigyan Ashram would also use the developed method to further their understanding of structural behaviour.

It was hoped that a reliable method of analysis would increase the number of potential uses of the structure and hence its market demand, benefiting both the community and the business that manufactures the dome, which was founded and run by an ex-student of Vigyan Ashram.

The objectives of this project may be summarised as follows.

1. The development of a method of finite element analysis for geodesic dome structures

using Microsoft Excel 2003. The program needed to provide a user friendly format that gave the user the opportunity to define a geometry, select appropriate material properties and apply a variety of loading conditions. It was required to output information about nodal displacements and forces in the elements.

2. The assessment of the dome joints used in the structure to determine their design limits. Based on these findings, a relationship between material parameters and the ultimate failure strength of the connections was to be developed.

3. The development of an additional spreadsheet that would allow the user to calculate all the relevant dome fabrication details - how many different struts are required, how long they are, how many bolts are required for sufficient connection strength etc.

Project timeline

This project was to be carried out over a period of 28.5 weeks - from the end of September through to mid-May. A Gantt chart breakdown of the project plan may be found in Appendix A, with all the major project deadlines highlighted.

Work was broadly categorised into three phases.

- Phase I: Initial research and planning; lasting from September through to January, culminating in the submission of the literature review. In this phase, background reading and discussion with Vigyan Ashram would lead to the development of a list of objectives and a project plan. Additionally, preparation work for the later tension testing work would be scheduled, including the submission of a risk assessment and the production of engineering drawings to fabricate the required dome joints.

- Phase II: Data collection; overlapping with Phase I, from December to the end of April. Here, experimental work would be carried out and the spreadsheets developed, culminating in the submission of a draft version of the final report.

- Phase III: Project conclusions; from April until the concluding oral exam in May. Upon return of the draft report from the project supervisor, modifications would be made and the final project submitted on the 29th of April. Additionally, a poster design for display in the department would be produced and preparation for the oral exams would occur in this period.

Contents

List of Tables

List of Figures

1 Introduction

The project plan included in the prelude of this report defines the project objectives agreed with Vigyan Ashram and the expected timeline in which they were to be achieved. The literature review provides context and background information to justify the need for this work and the theory section summarises the necessary information required to understand the FEA method developed in Excel.

The main body of the report covers three main aspects of the project.

1. The development of a geodesic dome model and the subsequent analysis of the dome using Strand7, a commercial FEA package, which provided an early basis for gathering results and a benchmark against which to compare the Excel based method.

2. The development of a relationship to predict the failure strength of the joints from the material properties and geometry, using a combination of physical tension testing and stress analysis.

3. An overview of the finite element (FE) method developed in Excel.

In the final part of the report, the success of meeting the objectives outlined in the project plan is discussed and conclusions are drawn, with recommendations for further work in this area.

2 Literature review

2.1 Introduction

The purpose of this literature review is to give context to the relevance and necessity of the work undertaken in this dissertation, and to introduce the concepts and definitions that will aid the understanding of the rest of the work herein.

Firstly, a brief history of the geodesic dome's role in the reconstruction and rehabilitation in wake of the 1993 Killari earthquake is given. The NGO that has ultimately continued to locally produce the dome kits to the present day, Vigyan Ashram, is then introduced. The work halted at the Water Bank project in 2005 is used to demonstrate the need for an assessment of the loading on the geodesic domes.

The second part of the literature review examines the definition of a geodesic dome and looks briefly at its history. The strengths and weaknesses of geodesic domes are discussed, and the modified version of the dome used by Vigyan Ashram is introduced.

Finally, the possible methods of braced dome analysis are reviewed and the decision to produce an Excel based program is justified. Previous work in this area is reviewed,

and the shortcomings are used to justify Vigyan Ashram's need for a bespoke structural analysis package.

2.2 Pabal

2.2.1 Earthquake and aftermath

The following description of the earthquake and aftermath are based upon extracts from the account of Professor Horst Rolly [Rolly, 2007], who lived in the region at the time of the quake.

In the early hours of the morning of the 30th September 1993, the Killari earthquake struck the Maharashtra province of India. The first quake lasted for 40 to 50 seconds, survivors recounting that houses "swayed like a cradle" before they caved in and buried people underneath. Animals, traditionally staying in rooms attached to houses, met the same fate. The magnitude of this disaster became apparent only days later; 7,928 human lives lost, a further 16,000 were injured and more than 15,800 livestock were killed. The damage was total in 52 villages of the Latur and Osmanabad districts, but the effects of the disaster were felt in more than 2500 villages in the 11 neighbouring districts.

Real poverty proved to be a blessing as the landless poor lived in thatched-roof buildings made of straw and reeds or split bamboo, finished with mud-plaster. These houses performed extremely well, suffering only minor cracks to the mud plaster walls. The structures that suffered most were those constructed of thick masonry to provide better insulation against the summer heat. Local builders reported that "... the failure of stone masonry during the earthquake was largely because of the excessive wall thickness demanded by the Maratha households for thermal comfort and storage of valuables within the thickness of the walls." No official engineering standards existed in rural Maharashtra before the quake; often boulders were piled upon shallow foundations, bonded only with minimal cementing. In normal conditions these constructions are relatively stable, but on the soft Black Cotton soil of the region they collapsed easily when the earth shook.

No early warning system for such a natural disaster was in place and no comprehensive disaster management plan existed before the quake. Regardless, the civic response was spontaneous. Able-bodied survivors assisted the injured and dug in debris to rescue the living and recover the dead with their bare hands as initially no excavation equipment was available. The Maharashtra state government in Bombay responded to the news immediately by sending helpers from civic bodies and doctors from neighbouring districts along with supplies. The Indian armed forces were brought in to aid with the rescue and relief operation, with some 10,000 troops bringing in lifting machinery, tents and water purification units. The press rushed to the scene, spreading word of the tragedy, ultimately leading to fund raising initiatives, both national and international. As more and more donations poured into government collection and distribution centres the authorities

became unable to handle them, until ultimately the Chief Minister publicly announced three days after the quake that "... no additional help of unsolicited kind is needed either in the form of items or volunteers... We already have much, so much."

For the longer term reconstruction effort, bilateral donations from the United Nations Development Program, the Asian Development Bank and a World Bank loan granted the Indian Government US$358 million as a low interest emergency loan with a 30 year payback period to add to its resources. In the third week of October 1993, the Government of Maharashtra invited NGOs for round table discussions of how to proceed with reconstruction efforts. The state government wanted to ensure that despite the large variety of agents involved in the reconstruction effort, the houses met common standards of earthquake safety. However, before the technological aspects of proposals could be fairly assessed, the Indian media reported that politicians were attempting to exclude certain designs: "... the chief minister and his cabinet colleagues are also believed to have taken the psychological aspect into account. Non-conventional structures like geodesic domes were ruled out because people are not used to living in them, it is learnt." [Indian Express, October 13th 1993]. By the time of the round table discussions, Adventist Development and Relief Agency (ADRA) India had already contacted the villagers of Gubal about the possibility of building geodesic domes as a safe housing device. The villagers agreed that a sample geodesic dome could be built at the resettlement site for the villagers to inspect and scrutinise. On the condition that the dome met village approval, the design would be adopted as a rehabilitation measure. The Gubal village elder ultimately submitted a request for 365 houses to be built, rather than the 182 originally planned.

2.2.2 Vigyan Ashram and engINdia

Early discussions of ADRA India with the people of Gubal concluded that safe housing was of paramount importance in the villagers' opinion. The horrifying experiences of the Killari earthquake had turned much of the village into a graveyard, and none of the surviving inhabitants wished to stay and live in old Gubal. After careful comparison of earthquake resistant architectural designs, ADRA India decided upon the geodesic dome. Vigyan Ashram, a research institution based in the village of Pabal had experimented with the geodesic dome for a number of years. Dr Kalbag, Vijay Kumar and other like-minded engineers based there developed a modified version of the dome called the "Pabal" dome, which was subsequently marketed by a number of entrepreneurial small scale industries, producing prefabricated components as part of low cost do-it-yourself kits and taking orders to build and maintain the domes. Vigyan Ashram has continued to manufacture and supply dome kits since the 1993 Killari earthquake, focusing on making low-cost, safe and comfortable housing that is affordable for the lower-middle class of both urban and rural populations.

As well as a research institution, Vigyan Ashram serves as a science centre for rural

youth. The centre was founded in 1983 by the late Dr Kalbag. Places are offered both to students in India's public high school system, and also to school drop-outs frustrated by conventional education. Vigyan Ashram's philosophy [Kalbag, 2004] places an emphasis of teaching science through practice; to experiment, measure and record data, to recognise patterns and to form and test hypotheses. The course is novel in two aspects: what it achieves through student input and how it benefits the village economy. Students undertake projects in numerous areas including water resource development, construction, workshop technology, energy, transport, environment agriculture, and home & health.

engINdia[1] is a partnership between 6 students from the University of Cambridge, Massachusetts Institute of Technology (MIT) and the Indian Institute of Technology Bombay. An expedition was conducted during the summer of 2005 to the area of Pabal, Maharashtra, where the engINdia team worked with Vigyan Ashram and the local community to gain an understanding and appreciation of the development issues concerning rural India which could be tackled through engineering.

Through this relationship, MIT have established a FAB LAB in Pabal through their "Bits and Atoms" program, with the intention of providing Vigyan Ashram and the local community the necessary tools to empower them to solve their own engineering problems. FAB LABs[2] share core capabilities, so that people and projects can be shared across them. The kit includes: a computer controlled lasercutter, a large scale milling machine, a signcutter, a micron resolution precision milling machine and programming tools for low-cost, high-speed embedded processors.

2.2.3 The Water Bank project

The Water Bank project is a recent rural housing project intended to house 40 families in Maharashtra. Work that began in January 2005 has been halted due to concerns over the loading applied to a series of geodesic domes which form a large portion of the whole complex. The domes have soil packed over them which was never anticipated in Vigyan Ashram's original design.

The complex is an experimental 8 million rupee investment (£116,000 at Jan 2009 rates) to house 40 families in Ankoli, Maharashtra. Of the 120 domes supplied to the Water Bank housing project 40 are planned to be subterranean and are therefore affected. The complex is intended to provide each of the families with a guaranteed 2,000 litre water supply year-round, a 300 square foot greenhouse, 350 square foot cave house, 900 square foot work area, a terrace, a courtyard and 0.5 acres of land. The intention of the project is to promote sustainable housing and fulfil the desires of the residents to be self-employed.

[1] http://www.engindia.net/
[2] http://fab.cba.mit.edu/

2.2.4 Structural analysis

When the Water Bank project halted, Vigyan Ashram and engINdia approached the student led charity Engineers Without Borders UK[3] to request that more research be conducted into the design of the geodesic domes manufactured in Pabal.

There is a clear need for a method to model the structural response of the geodesic or "Pabal" dome under various loading conditions. Vigyan Ashram's original brief requested that an assessment of the loading encountered by the domes should be performed and design alterations should be recommended to accommodate the expected loading.

Following discussions with Vigyan Ashram, it emerged that they wished to alter the original brief to focus the design of a bespoke structural analysis package. This would allow Vigyan Ashram to analyse the structural response of the domes in-house without the need for buying costly finite element software licences or requesting outsider help. This would be a further step to empower the locals to solve their own engineering problems in the future. An in-house analysis method would allow assessment of the dome's structural response in situations previously not considered. Vigyan Ashram hoped this would increase the number of potential uses of the structure and its market demand. If appropriate, students at Vigyan Ashram would also use the package to further their understanding of structural behaviour.

2.3 Geodesic domes

2.3.1 Buckminster Fuller

Engineers and architects have always held a special interest for structural systems that enable them to cover large spans with minimal interference from internal supports. It is perhaps no surprise then that dome structures, capable of encompassing maximum volume with minimum surface area, are one of the oldest structural forms and have been used in architecture since the earliest times. The earliest geodesic dome was designed and built in 1922 by Walter Bauersfeld in Jena, Germany [Makowski, 1979]. It was not until the 1950s, and largely due to the efforts of Buckminster Fuller, that the geodesic dome became a vogue form of design.

Buckminster Fuller was an American born in Massachusetts, USA. Though he never possessed formal qualifications in engineering or architecture, he influenced numerous architects and some engineers to a greater extent than many eminent members of their professions [Zung, 2001]. He filed for a patent in 1951 for an improved version of the geodesic dome design, which has since been used in structures such as the Tacoma Dome (WA, USA), Poliedro de Caracas (Caracas, Venezuela) and The Eden Project (Cornwall, UK).

[3] http://www.ewb-uk.org/

Buckminster Fuller's passion for geodesic structures came from the design's affinity with Nature, an effect he described as the "energetic-synergetic" geometry of his domes. "Energetic" refers to Fuller's belief that Nature always builds the most economic structures. He claimed that geodesic domes built upon principles embodying force distributions similar to those of atoms, molecules, and crystals, would form the lightest, most efficient forms of construction. Fuller defined synergy as the "integrated behaviours of nature and the behaviour of a whole system unpredicted by the behaviour of any sub-assembly of its components." For example, hydrogen and oxygen gases, when combined in the right conditions produce water, and this could not be predicted by the individual properties of either gas. Similarly, the geodesic dome exhibits a stiffness and rigidity greater than that predicted based on the sum of the individual components that make it.

2.3.2 Definition

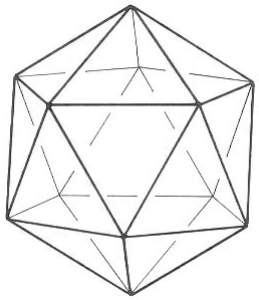

Figure 1: Isosahedron

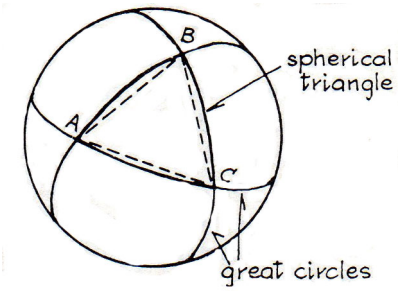

Figure 2: Great circles [Morgan, 1981]

Buckminster Fuller based his original design on the sphere division of an icosahedron, (see Figure 1) although geodesic domes have since been constructed using octahedron and dodecahdreon symmetry systems to circumvent Buckminster Fuller's patent. The aforementioned shapes are all part of the family of platonic solids - polyhedra made up entirely of congruent regular polygons. An icosahedron exploded onto the surface of a sphere produces twenty equilateral spherical triangles, the vertices of which may also be described by the intersection of three great circles (circles with a diameter equal to that of the sphere) and are referred to as geodesic points, such as A, B and C in Figure 2. Fifteen great circles also fully define the primary bracing of a geodesic dome. If the chords that join the vertices are straight lines rather than curves, planar triangles are formed and this creates the geodesic network commonly used in structures.

The primary bracing is truly geodesic, but impractical to use in most circumstances as members quickly develop excessive slenderness ratios as the diameter of the dome increases. To obtain a more regular network, a secondary bracing is introduced, modularly dividing each equilateral triangle into a number of subdivisions. There are two possible classes of geodesic subdivision; for Class I subdivision, the dividing lines are parallel to the

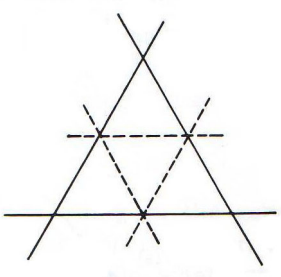

Figure 3: Class I sub-division [Motro, 1984]

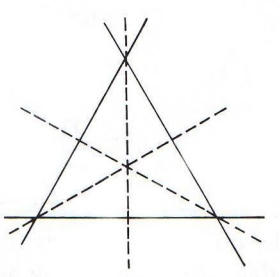

Figure 4: Class II sub-division [Motro, 1984]

edges of the primary bracing (Figure 3); in Class II, the dividing lines are perpendicular to the primary bracing (Figure 4). Class I subdivision produces geometry where the edges of the triangle lie on a great circle, which leads to simple design of a hemisphere with planar connections; this may not be achieved with a Class II subdivision. Class II subdivisions require a smaller number of bar lengths, which is advantageous for fabrication; however, the differences between individual bar lengths are resultantly greater in a Class II dome, and this produces a less uniform stress distribution. Additionally, Class II domes can only be achieved with an even frequency of subdivision.

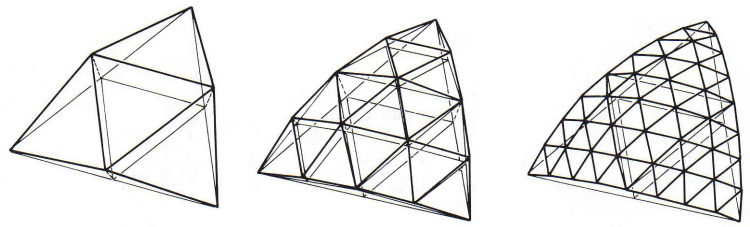

(a) V2 (b) V4 (c) V8

Figure 5: Example sub-division frequencies [Motro, 1984]

A subdivision, or "frequency" is defined by the number of triangles each edge of the primary bracing is divided into (Figure 5). The frequency is often referred to in short-hand as a number, with the prefix "V". It should be noted that if secondary bracing is introduced, the triangles are no longer perfectly equilateral - the bars forming the skeleton show variations in length, and the number of different lengths required to fabricate the dome increase with the frequency of subdivision.

Odd order frequency domes cannot produce a hemispherical shape, as an equatorial perimeter ring is only produced for even order frequencies. Odd order frequency subdivisions are nominally referred to with the suffix 3/8ths or 5/8ths, to indicate respectively if the ground ring is above or below the equator of the geodesic sphere.

2.3.3 Explanation of behaviour

The manner in which a braced dome behaves depends on the configuration of the members. Fully triangulated domes, such as geodesic domes have a high stiffness in all directions and are kinematically stable (no mechanisms) when idealised as a space truss. A dome which is not fully triangulated is not kinematically stable when idealised as a truss and stiffnesses may vary greatly in different directions on the dome's surface. While radial cable domes may exhibit greater stiffness to uniform loads, triangulated domes demonstrate greater stiffness to non uniform and concentrated loads [Kardysz et al., 2002].

The forces in a geodesic network are an equilibrated combination of tension and compression. Tension forces are global and continuous, while compression forces are local and discontinuous. Buckminster Fuller coined the term tensegrity, a portmanteau of tensional integrity, to convey the concept of coherence and resilient elasticity of geodesic networks.

Richter [1975] argues that the use of geodesic subdivision produces structures of greater strength than conventional braced domes. The triangle is a planar figure which has maximum rigidity accomplished with the least effort. Symmetrical triangular systems provide the most economic energy flow, and a geodesic network produces a structural form with self stabilizing properties.

2.3.4 Strengths and weaknesses

A dome is a typical example of a synclastic surface, where surfaces are of positive Gaussian curvature; i.e. where the curvature of any point is the same sign in all directions. Synclastic surfaces are not developable; i.e. they can not be flattened into a plane without shrinking or stretching of the chords. This is why in practice domes cannot be built from one uniform member size. However, Makowski [1965] points out that geodesic domes are exceptionally good in this respect; even for sizable spans only a small number of different bars sizes are required, making the structure ideal for optimising the manufacture of components and prefabrication. Morgan [1981] describes how the Kaiser Aluminium Company (USA) was one of the first companies to take out a full license under Buckminster Fuller's patent for a concert hall in Honolulu, Hawaii. The 44.2m dome was erected within 22 hours of the components arriving, and within 24 hours a concert was held at the venue by the Hawaiian Symphony Orchestra to an audience of 1832.

In high risk earthquake areas such as Japan, quake resistant designs have evolved through trial and error exercises over the centuries. Modern design guidelines have emerged from such empirical data; the rules listed below are extracts from a planning aid for architects and engineers [Dowrick, 1978] and are used to highlight some of the properties that make the geodesic dome a highly earthquake resistant design.

- The degree of compactness in a building correlates with its resistance against seismic shock. A hemispherical structure is the most geometrically possible compact form

of construction, enclosing maximum volume with minimum surface area.

- Reinforcing elements should be rigid and symmetrically organised, located close to the building boundary and distributed evenly throughout the structure; the geodesic skeleton does exactly this.

- The centre of gravity should be as low as possible. A dome has a lower mass point than any cuboid structure of similar proportions.

- The construction should be elastic and deformable to a certain extent, especially through the core grid. The geodesic dome exhibits this behaviour, and empirically has been proven to survive even severe earthquakes with only minor cracking in the cladding.

Geodesic domes produce extremely light skeleton structures that are very stiff and rigid, enclosing a large area without need for internal supports. Due to the light weight, the round shape of the dome perimeter, and the generally uniform load distribution of geodesic dome structures, deep foundations are not normally required. Construction of shallow foundations allow a considerable saving in time and money over deep foundations.

The geodesic dome is, however, not without disadvantages. One complaint is that the perimeter chords following the shape of an icosahedron produce an irregular or ragged line that may be objectionable on architectural grounds; the aesthetic appearance of the dome is largely dependent on how these closures are treated. The most common objections are functionalist; due to the hemispherical shape of the structure, effective sound isolation is difficult to achieve through partitioning of rooms, leading to a perceived loss of privacy. Furniture, unless custom made, also presents a problem due to the curved walls of the structure which can result in some loss of space.

2.3.5 The Pabal dome

Vigyan Ashram's Pabal dome design is a developed version of the basic geodesic dome structure. The Pabal dome is based on a V3 5/8ths Class I dome as shown in Figure 6.

The dome is made of prefabricated equal angle struts and disc hub joints made from mild steel. A house kit may normally be assembled in one day using only simple nut and bolt construction, without the need for specialised equipment. The kit requires no brick masonry, so is easy to transport. The finished skeleton structure is clad using multiple layers of chicken wire reinforcing mesh and ferrocementing (or "guniting") technology; a form of spray on concrete that is cheaper, lighter and faster than cladding using masonry.

The basic structure is a cost effective form of design, costing only RS.200/ft^2 (£9.21/m^2, January 2009). Domes can be interconnected to form interesting housing designs and add further rooms or space. The cladding forms an insulating thermal mass that keeps the house cool all year round.

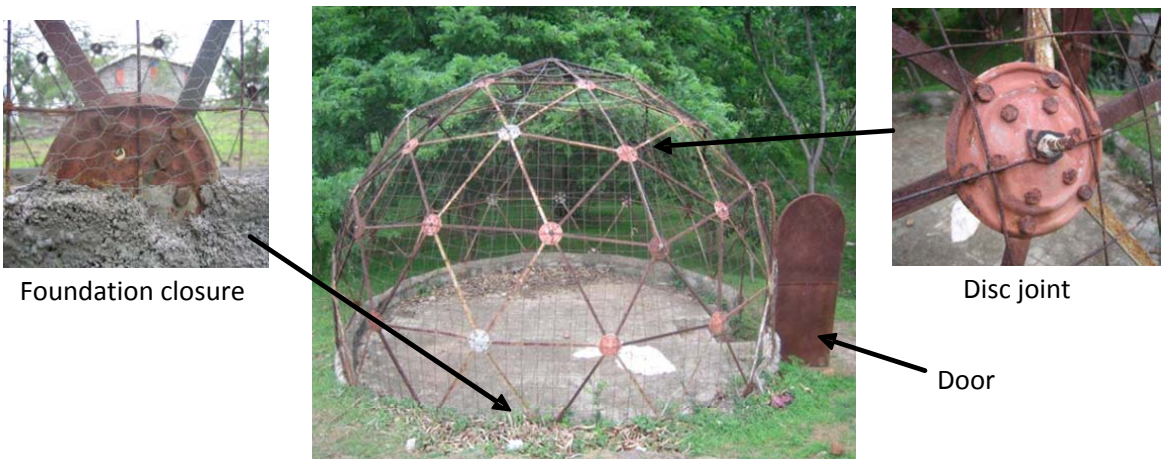

Figure 6: Pabal dome

2.4 Braced dome analysis

2.4.1 Idealisations

Mullord [1984] states that before any engineering structure can be analysed, it has to be represented by an idealised mathematical structure whose behaviour models sufficiently closely that of the original structure. Two idealised methods exist for braced dome structures: equivalent shell methods and discrete structure methods. The equivalent shell method may be divided further into two sub-groups - orthotropic shell theory and finite difference theory. Both methods use approximations which aim to smear the effect of discrete members uniformly over the surface of an equivalent shell, leading to a set of governing differential equations that are solved using a harmonic solution. The second group of methods allow the analyst to tackle the discrete structure directly. Again, this may broadly be split into two sub-groups[4]: space truss analysis, where all joints are assumed pinned, and space frame analysis, where joints are assumed continuous. Both discrete structure methods produce a large set of simultaneous equations that can only be feasibly solved with the aid of a computer.

Equivalent shell methods are best suited to early design work or for structures too large to be analysed discretely. Over the years, computers have become more affordable and more powerful, and the use of finite element analysis has become increasingly popular method of modelling structures that are too time consuming or complex to resolve by hand [Coates et al., 1988]. Vigyan Ashram favoured the development of a spreadsheet based discrete structure method, as such software is widely available and significantly cheaper than dedicated analysis packages. Matlab and C++ based FEA programs were alternatives also considered, but were ruled out due to the required presupposition of programming

[4]Other direct analysis methods do exist, for example, the equilibrium method discussed by Quintas and Avila [1993] or Endogenous force analysis [Burkhardt, 2007], but space frame and space truss idealisations are by far the most common.

knowledge in order to understand the workings of the structure stiffness method. It is important to understand that Vigyan Ashram's students will have limited programming knowledge due to the vocational-style training used there to teach. Microsoft Excel 2003, a widely available spreadsheet package that Vigyan Ashram are familiar with using, was mutually decided to be the most appropriate platform to develop the solution with.

2.4.2 Analysis

Discrete structure methods can be modelled using linear or non-linear analysis. Linear analysis assumes a linear stress strain relationship, and together with information about the material behaviour can be used to check for local member or joint failure. However, instability effects beyond the point at which the material yields require non-linear analysis to account for member effects such as plastic yielding. Non-linear analysis methods have been extensively studied by many authors [Meek and Loganathan, 1989], and are based on either the finite element method or on the beam-column approach.

To decide which analysis method was most appropriate, it was important to understand the level of complexity of the different methods. Non-linear methods are generally more technical and more computationally exhaustive, but produce a more accurate solution. However, a more accurate, more technologically complex method was not necessarily the most relevant technology for Vigyan Ashram to use. Vigyan Ashram required a straightforward analysis method that produces sensible design information for a comprehensive range of loading options. Linear analysis, being less computationally intensive and requiring less engineering knowledge to understand was therefore better suited for use in Excel.

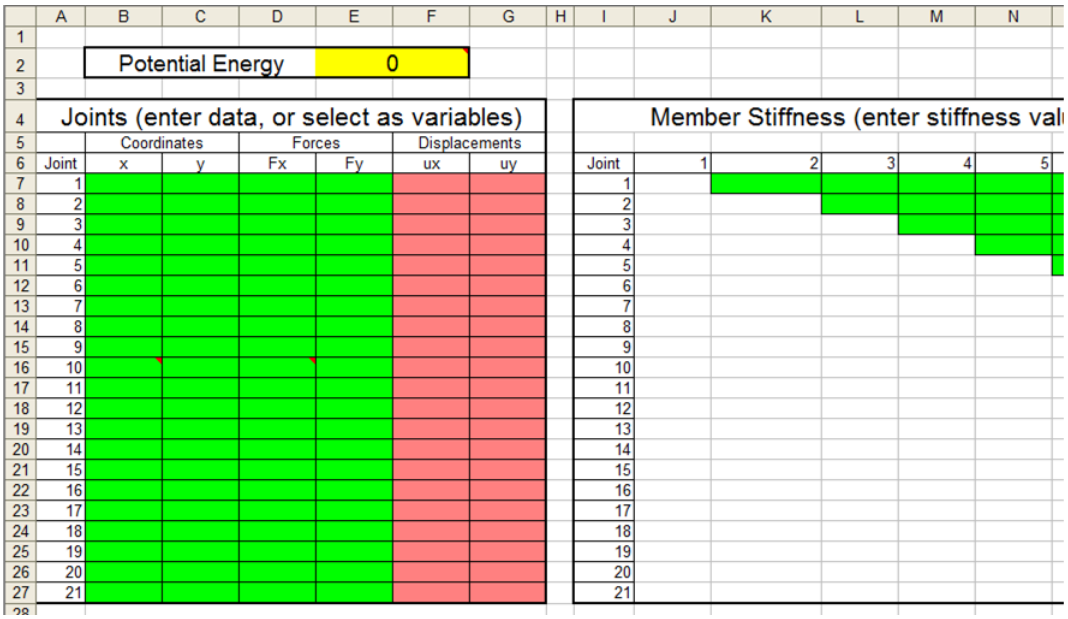

Figure 7: Brown University's 2D FE program

2.4.3 Previous work

The concept of using Excel for the purpose of structural analysis is not entirely new. Teh and Morgan [2005] highlight the benefits of the platform for teaching the stiffness method to final year university students at Curtin University of Technology, Australia. Similarly, a method of forming basic 2D pin jointed analysis developed by Brown University, USA[5] is available freeware for solving simple nodal applied loads (Figure 7).

However, these examples are limited to two dimensional analysis of a limited number of members. The interfaces are also at a very basic skeleton level - requiring the user to specify each nodal coordinate, member stiffnesses, fixities and each nodal load, resulting in a very time consuming and unnecessary data entry exercise. Some of these programs also make use of built in matrix manipulation functions that are not designed to work with large matrix problems. Vigyan Ashram's request was for a user friendly interface that would streamline the analysis process of a geodesic dome and work with a variety of different load situations. To achieve this, a fresh approach and a bespoke design were required.

3 Theory

The following section introduces the underlying theory required to understand how the FEA package covered in Section 6 was developed. The emphasis here is on the processes involved in forming and solving a system, rather than justification of why a particular method is most suitable (this is covered in Section 2.4).

The reader is assumed to have a grasp of matrix mathematics; understanding matrix addition, subtraction, multiplication, inversion and transposition[6]. A previous understanding of the stiffness method will be helpful, but is not essential.

3.1 Stiffness method

The stiffness method allows us to analyse a structure which is an arbitrary assembly of simple structural members by breaking down the components into "elements" (members) and "nodes" (joints). It can deal with a wide range of design situations, including space frame structures (where joints are treated as continuous). However, only the method for a space truss system needs to be discussed here for the reasons described in Section 2.3.3.

The basis of the stiffness method for a structure limited to pin jointed elements is that every member has analogous properties to those of a spring; that is, an axial load F may be applied to the end of a spring, and this is internally carried, causing a resultant change in length u.

[5] http://www.engin.brown.edu/courses/en3/notes/Statics/Structure_tutorial/Structure_tutorial.htm

[6] If not, most maths textbooks cover the topic of matrices; see for example Stroud [2001].

The relationship between applied load and the resulting displacement is a property of the element, known as a spring constant, or stiffness k (Equation 1), expressed as

$$F = ku \ . \tag{1}$$

It is possible to model the response of a structure by connecting together a system of individual spring elements and solving to determine the displacements. In order to find a structure's response to a known set of forces, a way of determining the stiffness of each member must be found. Though the derivation of element stiffness is quite elementary, it has been included to help explain the steps taken to post process the spreadsheet data in Section 6.4.1.

Intuitively, if the section is made larger, or a different material is used, the value of k will change. Consider the expressions for stress (σ) and strain (ϵ) in an element

$$\sigma = \frac{F}{A} \tag{2}$$

and

$$\epsilon = \frac{u}{L} \ , \tag{3}$$

where F is the axial force in the member, A is the area of the cross section, u is a resultant change in length and L is the length of the original member. Now, for a linear elastic material, these expressions may be related using Hooke's Law:

$$E = \frac{\sigma}{\epsilon} = \frac{F/A}{u/L} = \frac{FL}{uA} \ , \tag{4}$$

and rearranging gives

$$F = \frac{EA}{L}u \ . \tag{5}$$

Comparing Equation 5 to Equation 1, it is clear that an expression for the spring constant in terms of geometric and material properties of the material exists; $k = \frac{EA}{L}$.

Now that the stiffness for an individual element has been determined, the principle needs to be extended to work for a three dimensional system.[7] In 3D the expression relating forces and displacements is much the same, however a total of six degrees of freedom (DOF) must now be considered for each element, as each node can displace in three dimensions: u, v and w (Figure 8).

Rather than dealing with multiple linear expressions, it is convenient to express the local stiffness of an element using matrix notation:

[7]The reader may wish to follow a worked example for a 1D or 2D structure stiffness method from a textbook, such as Mullord [1984], before reading the remainder of this section.

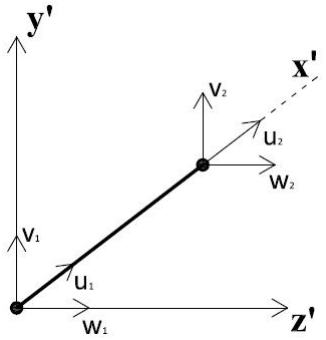

Figure 8: DOF for a pin jointed element in a local coordinate system

$$\begin{Bmatrix} f_{x'1} \\ f_{y'1} \\ f_{z'1} \\ f_{x'2} \\ f_{y'2} \\ f_{z'2} \end{Bmatrix} = \begin{bmatrix} \frac{EA}{L} & 0 & 0 & -\frac{EA}{L} & 0 & 0 \\ 0 & 0 & 0 & 0 & 0 & 0 \\ 0 & 0 & 0 & 0 & 0 & 0 \\ -\frac{EA}{L} & 0 & 0 & \frac{EA}{L} & 0 & 0 \\ 0 & 0 & 0 & 0 & 0 & 0 \\ 0 & 0 & 0 & 0 & 0 & 0 \end{bmatrix} \begin{Bmatrix} u_1 \\ v_1 \\ w_1 \\ u_2 \\ v_2 \\ w_2 \end{Bmatrix} \tag{6}$$

or, in shorthand form

$$\{f_{local}\} = [k_{local}]\,\{u\}\,. \tag{7}$$

Equation 7 uses a local, right-hand rule coordinate system x', y', z' (with the x' axis aligned with the direction of the truss element as shown in Figure 8). In a 3D structure, the local Cartesian coordinate system is unlikely to coincide with the coordinate system of the global axis X, Y, Z. In order to obtain meaningful stiffness matrix, a transformation matrix [T] is applied to the local stiffness matrix to obtain a common a global stiffness matrix for each element[8].

$$[K_{global}] = [T]^T[k_{local}][T]\ , \tag{8}$$

where

$$[T] = \begin{bmatrix} R_0 & 0 \\ 0 & R_0 \end{bmatrix}\ , \tag{9}$$

and the general form of R_0 is

[8]The derivation of this equation has been omitted, but is covered in Coates et al. [1988] and most good texts on FEA.

$$[R_0] = \begin{bmatrix} L_x/L & L_y/L & L_z/L \\ \frac{-L_xL_y\cos\gamma - LL_z\sin\gamma}{L\sqrt{L_x^2+L_z^2}} & \frac{\sqrt{L_x^2+L_z^2}\cos\gamma}{L} & \frac{-L_yL_z\cos\gamma + LL_x\sin\gamma}{L\sqrt{L_x^2+L_z^2}} \\ \frac{L_xL_y\sin\gamma - LL_z\cos\gamma}{L\sqrt{L_x^2+L_z^2}} & -\frac{\sqrt{L_x^2+L_z^2}\sin\gamma}{L} & \frac{L_yL_z\sin\gamma + LL_x\cos\gamma}{L\sqrt{L_x^2+L_z^2}} \end{bmatrix}, \tag{10}$$

where L is the length of the member, and its projected lengths on each of the global axes X, Y and Z are L_x, L_y and L_z respectively. The angle γ is a rotation of the element about the x' axis in Figure 8 to align the cross section of the element. In the case of a pin jointed (truss) structure, the shape and orientation of the cross section is unimportant as bending moments are ignored. Hence, for a space truss, $\gamma = 0$ and Equation 10 simplifies to

$$[R_0] = \begin{bmatrix} L_x/L & L_y/L & L_z/L \\ \frac{-L_xL_y}{L\sqrt{L_x^2+L_z^2}} & \frac{\sqrt{L_x^2+L_z^2}}{L} & \frac{-L_yL_z}{L\sqrt{L_x^2+L_z^2}} \\ \frac{-L_z}{\sqrt{L_x^2+L_z^2}} & 0 & \frac{L_x}{\sqrt{L_x^2+L_z^2}} \end{bmatrix}. \tag{11}$$

Once every element stiffness matrix has been transformed into a global coordinate system, it only remains to assemble all the matrices to form the structure stiffness matrix.

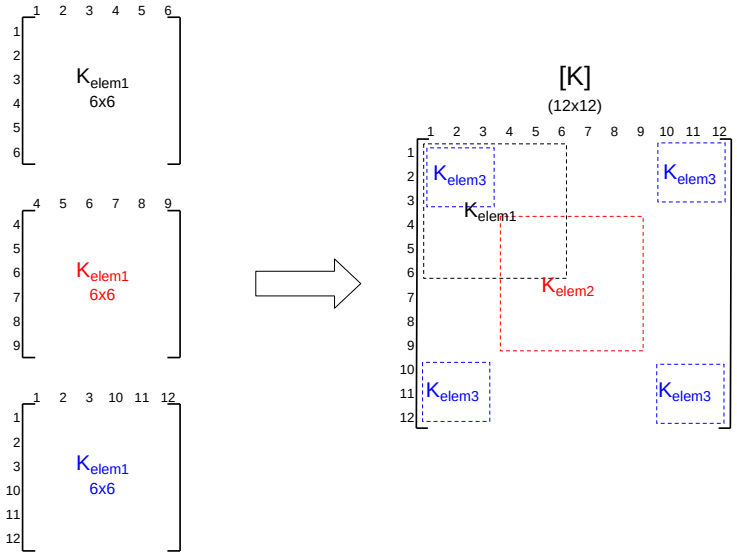

Figure 9: Assembly of the structure stiffness matrix from element stiffness matrices.

In FE programs, this is often achieved through the use of a steering matrix which links the local numbering scheme to the global numbering (see Figure 9). Nodes that are shared between elements will have overlapping contributions to the same cells of the stiffness matrix.

For a truss, each element stiffness matrix is 6×6 and the final structure stiffness matrix size [K] is determined by the number of nodes multiplied by the number of degrees of freedom per node. For example, the structure stiffness matrix in Figure 9 would have

to be composed of four nodes, as 4×3DOF produces the 12×12 matrix shown.

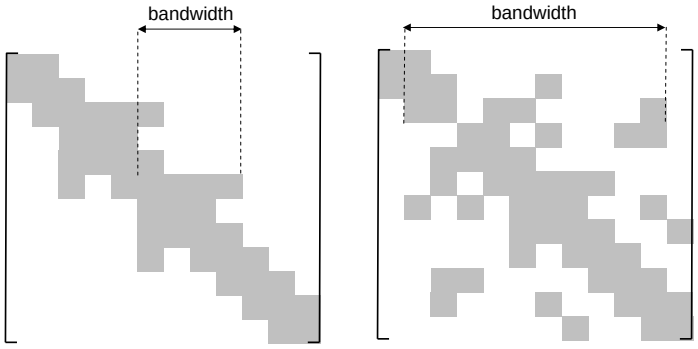

(a) Low bandwidth (b) High bandwidth

Figure 10: Structure stiffness matrix bandwidth

The node numbering system used in the structure is often critical to the efficiency of the solver, especially for large structural problems with thousands of elements. An efficient numbering system will produce a narrowly banded set of values on the leading diagonal of the populated matrix. The greatest width of any row in the matrix is termed the "bandwidth". A less efficient numbering system produces a much wider spread of results symmetrically about the leading diagonal and therefore produces a larger bandwidth (see Figure 10).

Finally, a matrix version of Equation 1 has been developed, in terms of a known global force vector $\{F\}$ and the structure stiffness matrix $[K]$

$$\{F\} = [K]\{U\} \ . \tag{12}$$

3.2 Solution methods

In order to gain a useful output from Equation 12, a method of solving it is required. First, boundary conditions are applied to the problem to define it uniquely. This is normally achieved through fixing certain degrees of freedom in the structure to represent anchorage to the ground.

Solving Equation 12 is not as straightforward as it may seem, as division is not possible in matrix algebra. The closest equivalent matrix operation that emulates division is to find its inverse $[K]^{-1}$, where

$$[K][K]^{-1} = [I] \ , \tag{13}$$

and [I] is an identity matrix, the matrix equivalent of unity. This allows us to then solve Equation 12 as

$$\{u\} = [K]^{-1} \{F\} \ . \tag{14}$$

However, for a large matrix, the process of inversion is computationally intensive and slow. Rather than tackle the inversion directly, considerably more computationally efficient methods are used. Trevelyan [2007] categorises solvers into two groups.

- **Direct solvers**. These solvers use methods such as Gaussian elimination and LU decomposition and are guarenteed to arrive at a solution if the matrix is non-singular. The number of floating point operations required to solve a system using a direct solver increases with the cube of the number of equations, meaning that for large matrix FE models, the solver quickly becomes a dominant part of the run time. Direct solvers also suffer from an accumulation of round-off errors.

- **Iterative solvers**. These solvers, such as the conjugate gradient method, make an initial guess and progressively iterate towards a solution until a convergence tolerance is reached.

Many of these methods may be found in mathematical textbooks[9], however only Gaussian methods will be mentioned in more detail here. Gaussian elimination has variants such as Gauss-Jordan elimination which has its own advantages and drawbacks.

The standard method, according to Kreyszig [2006], is a popular way of solving linear systems, based on a systematic process of elimination in the rows of the matrix in order to reduce the system to triangular form, as then the system may easily be solved by back substitution. As Gaussian elimination is a particularly well documented way of solving linear systems, it is unnecessary to reiterate the method in great detail here.

3.3 Post processing

Once the displacement vector in Equation 12 has been found using a method described in Section 3.2, it is a relatively straightforward process to obtain the internal axial forces that form an equilibrium with the externally applied force vector.

First, the transformation matrix from Equation 9 has to be applied to the global displacement vector in order to revert the displacements to the local coordinate system:

$$\{u_{local}\} = [T] \{U\} \ , \tag{15}$$

The difference between the x' directional nodal displacements $u_2 - u_1$ (see Figure 8) give the overall change in length of the element which is then used to calculate the strains, stresses and forces using Equations 2 and 3. A positive change in length indicates the element is in tension, a negative change indicates compression.

[9]See for example Kreyszig [2006].

3.4 Lateral earth pressure

The importance of the forces transmitted through the soil skeleton from particle to particle was recognised in 1923 when Terzaghi presented the principle of effective stress, which applies only to fully saturated soils [Craig, 2004]. For a horizontal soil mass with the water table well below the point of interest, the pore water pressure is zero, and hence effective and total vertical stresses at a depth below the surface, z, are equal and equivalent to the weight of all material per unit area above that depth:

$$\sigma'_v = \sigma_v = \gamma_{sat} z \ , \tag{16}$$

where σ_v is the total normal (vertical) stress on the soil mass, σ'_v is the effective normal stress, γ_{sat} is the bulk unit weight of the soil and z is the depth below some datum line at the surface of the soil.

To relate the distribution of vertical stresses to those induced horizontally against a retaining structure, Rankine's theory of earth pressure is used, which considers the state of stress in a soil mass when the condition of plastic equillibrium has been reached, i.e. when shear failure is on the point of occurring throughout the mass.

According to Rankine, vertical stresses in the soil remain at a constant geostatic value, wheras horizontal stresses increase or decrease depending on the local movements of the soil. In an active pressure zone, the retaining wall is pushed away from the soil mass in response to the action of the soil. In the passive zone, the retaining structure is being pushed against a resisting soil mass.

Rankine found that the relationship between the horizontal and vertical stresses in the active region[10] of the soil were related by an active pressure coefficient K_a, controlled by the soil's intrinsic shear strength parameter ϕ:

$$\sigma_h = K_a \sigma_v \ , \tag{17}$$

where

$$K_a = \frac{1 - \sin\phi}{1 + \sin\phi} \ . \tag{18}$$

4 Geodesic dome analysis

4.1 Introduction to Strand7

A commercial FEA package called Strand7[11] was used to build up an initial geodesic dome model. Strand is a general purpose finite element analysis system, used in a wide range

[10] The passive case calculation has been omitted for the reasons discussed in Section 4.3.3.

[11] http://www.strand7.com/

of applications in mechanical, civil, structural, aeronautical and biomedical engineering. The package was chosen because it was the most appropriate general purpose structural analysis software available at Durham University's School of Engineering.

While a powerful analysis tool, Strand would not itself be an appropriate piece of software for Vigyan Ashram; licensing costs for this software are high, and it operates a black box approach to analysis. The user is required to define a model and run the solver without guidance or explanation. Strand will then produce a solution, assuming the model is defined correctly, without showing the intermediate calculation steps. It therefore is not suited to teaching or explaining the FE method. However, to a competent user with a good understanding of the theory behind the program, it is an efficient tool for modelling the behaviour of structures.

The following sections describe the generation of geodesic geometry in Strand, the forces that were considered to act on the structure, and the results that it produced under various analyses.

4.2 Coordinate generation

The mathematical determination of geodesic dome coordinates may be achieved in one of two systems: Cartesian (presented by Davis [2007]) or polar (presented by Kenner [2003]).

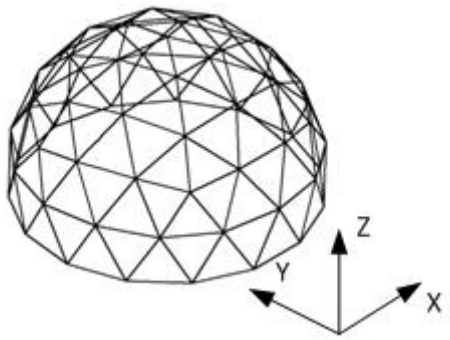

Figure 11: Global coordinate system used for analysis

A polar coordinate system defines the position of a coordinate relative to the origin at the centre of a sphere by a radius r and two angles θ and ψ, using algorithms based on formex algebra (see Sanchez-Alvarez [1984]). It is a system particularly suited to generating spherical geometries. However, a right-hand-rule Cartesian based coordinate system was used for developing the Strand model, as the stiffness method discussed in Section 3.1 is based upon Cartesian transformations. All forces and displacements in FEA are expressed in Cartesian form, and element stiffnesses are described locally and globally by Cartesian coordinates. It was hence logical that the basis of the model should be defined using a global Cartesian system (Figure 11).

A trial version of a package named CADRE Geo 6.0[12] was used to generate the geodesic geometry for the Strand model. CADRE is a design utility for generating a wide variety of geodesic and spherical 3D wire frame and surface models for Computer Aided Design (CAD) and FEA applications. In addition to generating coordinate data, the package was able to produce dfx files that could be imported directly into Strand, saving a considerable amount of time on assembling the elements connecting nodes manually. Setting the radius of a V3 5/8ths dome to unity in CADRE produced a set of coordinates which could be scaled to define the geometry of the dome for any radius in a spreadsheet.

When designing a structure, the internal floor area produced may be of greater concern than the overall external dimensions of the structure. This was indicated to be the case for Vigyan Ashram, as the Pabal Dome's assembly guide initiates the dome construction by marking the desired dome radius at perimeter ring (floor) level. Normally, the radius is defined at the equator of a sphere, but, as discussed in Section 2.3.2, an odd order frequency dome does not produce an equatorial perimeter ring because the structure is not an exact hemisphere. CADRE presented an option to expand the perimeter ring of the dome to equal the radius of the structure by applying a scaling factor to the coordinates (found to be 1.016). This factor was implemented as an option in the coordinate generation spreadsheet.

4.3 Loading

This section discusses the different loads that could act upon a geodesic dome structure, explaining which were considered important and why. The method that nodal forces were calculated from the applied loads is also described here. The totality of possible actions on the structure were considered to be: self weight, wind, snow, soil, imposed, seismic and impact.

4.3.1 Seismic and impact loads

It has already been demonstrated that the Pabal dome is an earthquake resistant form of design (Section 2.3.4). Additionally, impact damage was considered very unlikely given the residential use of the structure and that compound walls are often built around Indian housing [Rolly, 2007]. As it was not therefore necessary to consider these actions for normal design situations, it was assumed dynamic load effects were beyond the scope of this project and could be neglected from the analysis.

4.3.2 Snow

Snow loading is often critical to dome design [Knebel et al., 2002]. However, the Maharashtra region of India maintains a temperature of 20-30°C all year, and has a record

[12] http://www.cadreanalytic.com/cadregeo.htm

coldest day of 10°C [MapXL, 2006]. It was therefore safe to assume that snow loading would not be a design issue and could also neglected from the analysis.

4.3.3 Soil

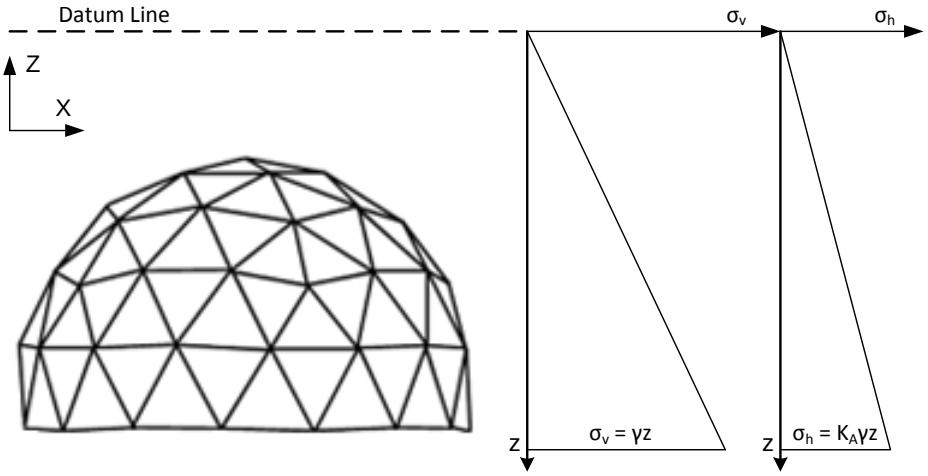

Figure 12: Horizontal and vertical stresses acting on a subterranean dome (after Landry [2002])

Soil loading was a necessary consideration because of the dome's subterranean use in the Water Bank project (see Section 2.2.3). It was assumed that the loaded dome would act as a retaining structure against any soil piled against it.

In order to calculate the forces upon the structure, Rankine's earth pressure theory (covered in Section 3.4) was applied to calculate the total horizontal and vertical stresses induced by the weight of the soil, based on a depth z below a user defined datum soil level, as shown in Figure 12. The surface area of the dome was then divided between the nodes, allowing the calculated stresses to be converted into nodal forces.

The stresses were calculated for an active pressure case, with no resistive mass of soil acting passively. It was conservatively assumed that the soil loading would be carried by the dome framework alone, as this reduced the complexity of calculating horizontal pressures for asymmetric loads.

The design assumes that the water table is below the foundations of the dome, which was a reasonable assumption to make as the region is prone to drought [Infobase, 2000]. This meant that underground aquifers were likely to be relatively deep below ground level, so that pore water pressure would not make a contribution to the stress state of the soil as described in Section 3.4. It was assumed that even during the monsoon aquifers would not recover to a level above the foundations.

The predominant surface deposit of the region surrounding Pabal village is Black Cotton soil, as shown by the regional soil map in Figure 13 [Shroff and Shah, 2003]. This is formed from the subaqueous decomposition or in situ weathering of basalt rocks, which

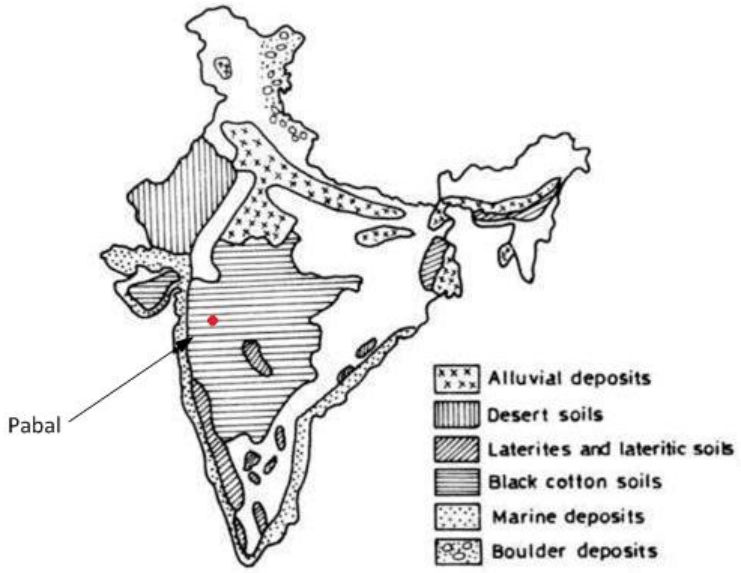

Figure 13: Regional soil deposits of India (after Shroff and Shah [2003])

produces the mineral Montmorillonite in an alkaline environment. Montmorillonite is a dark swelling clay commonly known in India as Black Cotton soil, due to its prosperity for growing cotton [Ranjan and Rao, 2000]. The load contribution due to the soil in the analysis (Section 4.5) assumed that the dome was buried in Black Cotton soil. In later work developing the Excel spreadsheet, more soil types were added as options for analysis.

4.3.4 Wind

Bhandari et al. [2003] give general guidance to the treatment of cyclonic storms and hurricanes, which are characteristic of India, especially during the monsoon season. They state that cyclonic storms do not normally extend further than 60km from the coast and that hurricane actions normally occur in the north east of India. This places Pabal (which is around 100km from the west coast) in a relatively low risk area.

The basic wind speed and design wind pressure were determined to Indian Standards using IS875:Part 3 [Bhandari et al., 1987]. These were chosen in preference to Eurocodes as they are more representative of Indian wind conditions (for example, they include factors of adjustment that account for cyclonic wind speeds). The design wind pressure p_d for the Pabal region was determined to be $0.584kN/m^2$, the calculations and assumptions behind this value may be found in Appendix C.

It was conservatively assumed that the wind pressure acts only from one direction and positively. In actual fact, the external pressure profile of a spherical structure is partly negative (i.e. suction) for angles between approximately 45° and 135° relative to the wind direction, which would act to reduce load on individual elements (see Figure 14). Stabilising wind pressures produced at the back of the dome due to vorticies were ignored.

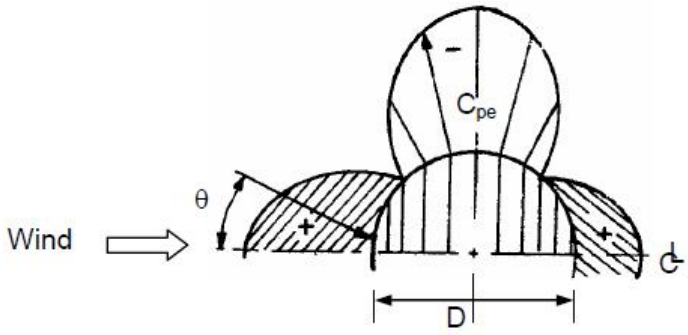

Figure 14: External wind pressure coefficients for a spherical structure (from Table 18, Bhandari et al. [1987])

For simplicity, forces on individual members were not considered; rather, forces were considered to act on the structure as a whole.

In order to get the total wind load acting on a particular building, a force coefficient based on the geometry of the structure was used. Together with the effective face area A_e and design wind pressure p_d this gave

$$F_w = C_f A_e p_d \, . \tag{19}$$

For a rough spherical structure, Table 20 of IS875 gave the force coefficient as $C_f = 0.7$. The effective area was taken to be projected area of the dome facing the wind, which in turn was a function of the dome geometry. The total wind loading on the face of the dome (found with Equation 19) was proportionally divided between the nodes by projected area to obtain the forces on individual nodes.

4.3.5 Self weight and imposed loads

The main components that contribute to the weight of the structure are the elements and the ferrocrete shell. These were initially represented using truss elements and plate elements with specified densities in conjunction with Strand's gravity function. This automatically calculated the nodal force contribution when an analysis was run.

This arrangement was convenient for use in Strand, but was discarded in favour of a spreadsheet based equivalent for two reasons; first, to ensure the method of generating forces would be common for Strand and Excel, so that results would be directly comparable; and second, because including plate elements in the analysis adds to the rigidity of the dome. Though this may appear beneficial, FE analysis of plate elements is a considerably more complex procedure than the analysis of truss elements. It was desirable to keep the analysis simple and focused on the geodesic skeleton. Aside from making the spreadsheet stiffness solver easier to follow, this also allowed the dome to be considered in situations

where it may not be built with a reinforced concrete shell, for example, when providing the framework for the greenhouses mentioned in the Water Bank project complex (see Section 2.2.3).

In order to divide the self weight of the structure between the nodes in an equivalent way to Strand's gravity method, the area supported by each node had to be calculated.

The shell was assumed to be approximated by loaded triangular plates; hence each triangle was bisected to evenly split the plate load distribution between the nodes. For the V3 5/8ths dome, three unique chord lengths A, B and C make up the possible triangle sizes for any given geometry. It was therefore possible to determine the area of each triangle, and, as each triangle was supported equally by three corner nodes, a third of the load on each plate was allocated to each node.

A similar, but simpler method was applied to find the distribution of member forces between nodes; assuming element homogeneity, then simply half the length of each connecting member is supported by the node under inspection.

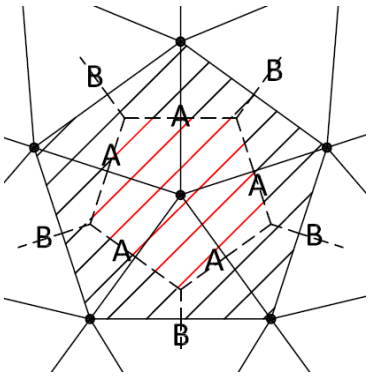

Figure 15: Example area division for a node

For example, in Figure 15, the node under inspection is bordered by five triangulated sets of elements, each consisting of two element lengths; two of A and one of B. The area of each plate in this case is $\frac{1}{2}AB$, and hence the total applied force on this node due to the shell would be

$$F_{shell} = 5 \times \frac{1}{3} \times \left((\frac{1}{2}AB) \times \rho_{shell}\, g\, t \right) \ , \tag{20}$$

where t is the thickness of the shell, ρ_{shell} is its density and g is acceleration due to gravity. All 5 members connected to the inspected node are of length A in this example, hence the nodal applied force due to the elements' self weight would be

$$F_{elem} = 5 \times \frac{1}{2} \times (A \times A_{elem}) \ , \tag{21}$$

where A_{elem} is the cross sectional area of the members.

Once these equivalent support reactions for all nodes were calculated, the sum of reactions in Strand for an isolated self weight load case was compared to those determined

in Excel to confirm that they coincided.

More components of self weight, including mesh density and joint weight were later included using the same distribution method to allow a greater amount of flexibility designing the structure. The imposed loading cases were similarly calculated.

4.4 Assumptions

In order to analyse the V3 5/8ths, Class I, Icosahedron based Pabal dome (with 61 nodes and 165 elements), and based on some of the considerations discussed previously regarding modelling forces on the structure, the following assumptions were made for the analysis.

- The good practice guidelines outlined in Eurocode 3, Section 5.1 apply.

    1. Analysis shall be based upon calculation models of the structure that are appropriate for the limit state under consideration.
    2. The calculation model and basic assumptions for the calculations shall reflect the structural behaviour at the relevant limit state with appropriate accuracy and reflect the anticipated type of behaviour of the cross sections, members, joints and bearings.
    3. The method of analysis shall be consistent with the design assumptions.

- The structure's working life was assumed to be 50 years (category 4, EC0-30, Table NA2.1), and the assumed building use was residential (category A).

- The door (see Fig. 6) and any windows in the dome structure were sufficiently spaced and installed in such a way that they would not reduce the structure's rigidity.

- The analysis was not rate dependent, i.e. time related effects on the structure, such as creep, were ignored.

- The boundary conditions assume that the structure was fully fixed at all its nodes at ground level.

- Members were assumed to be their correct mathematical geodesic lengths, so that no stresses were induced due to mismatched lengths.

- Any beneficial contribution to the structure due to a stressed skin effect from the reinforced ferrocrete shell described in Section 2.3.5 was ignored.

- The components that make up the structure were homogenous and isotropic.

- The analysis was static (where conditions are independent of time, as opposed to dynamic, which would consider behaviour under time varying conditions, such as earthquakes).

- The structure was modelled as a space truss; assuming that all joints were pinned. This was a reasonable assumption to make, for the reasons discussed in Section 2.3.3.
- The members were assumed to be sufficiently squat so that buckling effects could be neglected.
- The analysis was isothermal (independent of temperature).

4.5 Analysis

The dome analysis was completed in Strand based on the assumptions listed in Section 4.4. The purpose of the analysis was to explore which load cases were the most significant and to provide some solutions to which the Excel based FE method could be compared to for accuracy.

The dome was set to a radius of 3m, with its base expanded to equal the radius (see Section 4.2), as this is one of the most common kit configurations used at Vigyan Ashram.

Five load cases, described below, were considered individually and then in combination, using the recommendations for safety factors supplied by the British Standards Institution (BSI) Eurocode[13] 0: Basis of Structural Design [BSI, 2007].

4.5.1 Load Case I: Self weight

Based on the technical drawings contained in Rolly [2007] and the information provided by Vigyan Ashram, the thickness of the ferrocrete shell was estimated to be 50mm, bedded on two grades of reinforcing mesh; a coarse (gauge-19) square welded mesh and three layers of finer (gauge-18) 1" chicken wire mesh[14].

The joints and elements were assumed to be fabricated from mild steel. A nominal mass of 1kg was specified for the joints, and the truss elements were assumed to be $25 \times 25 \times 3$ equal angle sections made from rolled steel[15]; a choice reflecting the most common member type used by Vigyan Ashram.

The properties of these structural components are summarised in Table 1.

4.5.2 Load Cases II & III: Soil

Two soil load cases were investigated (Figure 16). The first assumed the soil would be buried uniformly around the dome up to its tip, which for a dome with a radius of 3m is a depth of 3.59m[16]. The second considered a case of non-uniform burial, a more realistic situation where only half the dome was buried under a soil mass.

[13]Eurocodes will henceforth be abbreviated to "EC" and will always refer to BSI [2007].
[14]Ferrocrete associated data from Hartog [1984].
[15]Steel data from Cobb [2007].
[16]Recall that odd order frequency domes are not hemispherical (Section 2.3.2), and hence the height of the dome is not equal to the radius.

Table 1: Element and joint properties

Material Parameter	Symbol	Value	Unit
Steel unit weight	γ_{steel}	77.2	kN/m^3
Young's modulus	E	200	GPa
Element cross section	A_{elem}	157	mm^2
Ferrocement unit weight	γ_{shell}	22	kN/m^3
Thickness of ferrocement	t_{shell}	50	mm
Mass of coarse mesh	m_c	1.15	kg/m^2
Mass of fine mesh	m_f	0.93	kg/m^2
Joint mass	m_j	1	kg

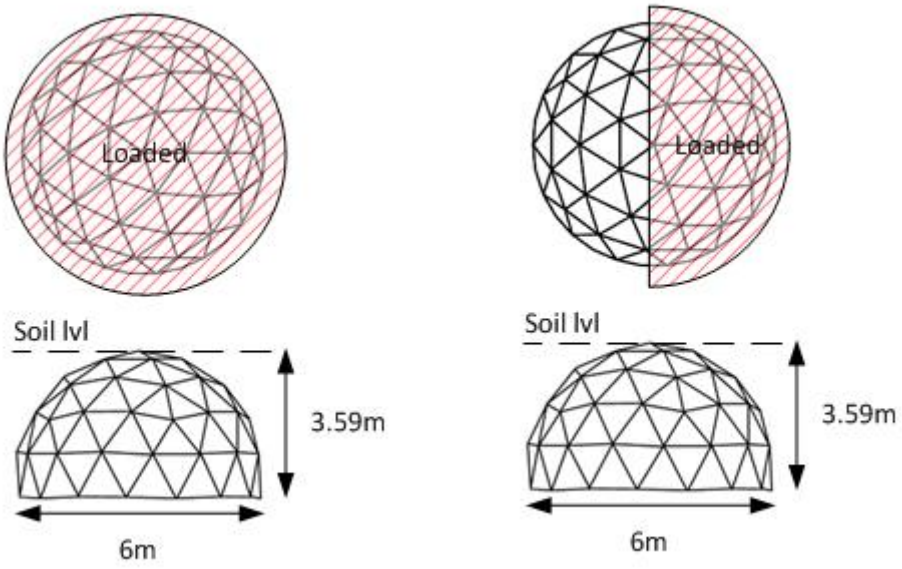

(a) Load Case II: full burial

(b) Load Case III: half burial

Figure 16: Soil loads considered

In both cases the soil used was assumed to be the regional topsoil: Black Cotton, with the parameters[17] summarised in Table 2.

4.5.3 Load Case IV: Wind

The wind load case on the structure was calculated following the assumptions described in Section 4.3.4. The prevailing wind direction was assumed to coincide with the global X direction (Figure 11). Using Equation 19, the face wind force to be applied was

$$F_w = 0.7 \times \left(\frac{5}{8}\pi 3^2\right) \times 0.584 = 7.22kN \ . \tag{22}$$

[17]Data based on the information provided by Ranjan and Rao [2000].

Table 2: Black Cotton soil properties

Parameter	Symbol	Value	Unit
Shear angle	ϕ	22	degrees
Bulk unit weight	γ_{bulk}	20	kN/m^3
Active pressure coeff.	K_a	0.455	

4.5.4 Load Case V: Imposed

A vertical imposed load of $0.6kN/m^2$ was allowed for. This was a sensible value for roof maintenance access, allowing for two workmen with tools to work on the roof.

4.5.5 Combination load cases

Three combination cases were considered, based on the safety factor recommendations for permanent and temporary loads on structures set out in EC0.

1. Combination I: This was chosen to model a simplified case of full subterranean usage of the dome. The full soil loading and self weight cases were factored as permanent loads, and imposed loading was factored as a primary case temporary load. Wind loading was ignored, as the dome would not be exposed to any wind.

$$\text{Combination I} = 1.35(\text{Case I} + \text{Case II}) + 1.05(\text{Case V})$$

2. Combination II: This modelled a more realistic case of subterranean usage, where the dome may be thought of as buried in part of an embankment. Imposed loading was assumed to be the primary temporary load, wind on the exposed face of the dome a secondary temporary load.

$$\text{Combination II} = 1.35(\text{Case I} + \text{Case III}) + 0.75(\text{Case IV}) + 1.05(\text{Case V})$$

3. Combination III: This model reflected a more general usage of the dome structure. The case considers the only permanent load to be the self weight of the structure. Since the structure would be fully exposed to the elements, it was decided that wind would be the primary temporary load. Workers accessing the roof would be a rare occurrence, so imposed loading was factored as a secondary temporary load.

$$\text{Combination III} = 1.35(\text{Case I}) + 1.05(\text{Case IV}) + 0.75(\text{Case V})$$

4.5.6 Results

The results of the Strand analysis are shown in Table 3. In the case of the maximum displacements, u_s, the global axis direction in which the displacement acted is specified after the number.

Table 3: Strand analysis results

Case	Max. Axial Forces (kN)		Max. Disp. (mm)
	Tensile	Compressive	u_s
Case I	4.2330	3.0366	-0.8961 (Z)
Case II	10.3014	69.7234	-6.8791 (Z)
Case III	33.3680	102.4470	7.8199 (X)
Case IV	1.0611	1.1811	0.2248 (X)
Case V	2.1608	1.5500	-0.4571 (Z)
Combination I	21.8374	99.5681	-9.9609 (Z)
Combination II	39.6312	143.9120	-13.0223 (Y)
Combination III	7.7368	5.9753	-1.5109 (Z)

4.5.7 Discussion

Several conclusions can be drawn from this basic analysis. Firstly, there is a clear indication as to why the geodesic dome structures are failing in the Water Bank project; the soil loading cases produce displacements an order of magnitude greater than for the other cases. Similarly, the compressive forces in the members are considerably larger, which indicates that premature failure of members and joints could be expected.

Under normal design conditions, the geodesic structures were found to deflect very little. Even under Combination III, the factored deflections and axial forces remain low for such a sizable structure.

An intuitive observation was that a symmetrical load (such as in Cases, I, II and V), produced a symmetrical distribution of forces in the members. Perhaps not so intuitive was that asymmetric loads produced much larger member forces. This can be seen clearly from comparing Cases II and III: the former is buried with twice the volume of soil of the latter, yet it is the asymmetric load case that develops considerably larger axial forces. This supports the findings of Pakandam and Sarshar [1993], where a similar analysis was carried out using snow loads.

It was also observed that the magnitude of the compressive forces exceed those of tensile forces predominantly in the soil load cases. This makes logical sense, as large external forces are acting to squash the dome inward, which would be expected to induce larger compressive forces inside the geodesic network.

5 Joint testing

5.1 Introduction

This section of the report describes how a relationship between the disc-joint properties and the ultimate failure load of a joint was developed.

To validate the structural stability of a post-analysis dome, it was necessary to know

whether the axial forces calculated would lead to failure of the joint. The connections used by Vigyan Ashram are discs rather than lap joints, which meant that the Eurocodes for connection design did not offer a method of estimating their capacity, as the code only provides a relationship for joints with a constant cross section.

In order to develop a parameter linked relationship, a dimensional analysis was performed, identifying dimensionless groups of parameters that required further investigation (the benefits of this are discussed in Section 5.3). These parameters were then investigated using both physical and computational testing:

- Some joint replicas were fabricated in-house at Durham University and tested to destruction to produce some "real life" data.
- Computational models of the discs were developed, testing a large number of configurations using stress analysis in Strand.

5.2 Pabal disc joints

Figure 17: Close up of Pabal dome joint

The joints used by Vigyan Ashram are stamped discs or "hubs" which have an array of pre-drilled holes to which the truss elements of the structure are bolted to, as shown in Figure 17. Two[18] different types of joint are required to build any geodesic dome configuration - those that connect six elements ("hexagonal" discs) and those that connect five elements ("pentagonal" discs).

[18] Arguably four-noded connections are needed for the ground level perimeter ring, however these can effetively be produced by using only four of the six connections on a hexagonal disc.

The discs are fabricated from scrap mild steel, using a fly press which stamps them into the correct shape, including two distinctive crimps, which add bending strength to the disc and also aid with stacking for storage and transport.

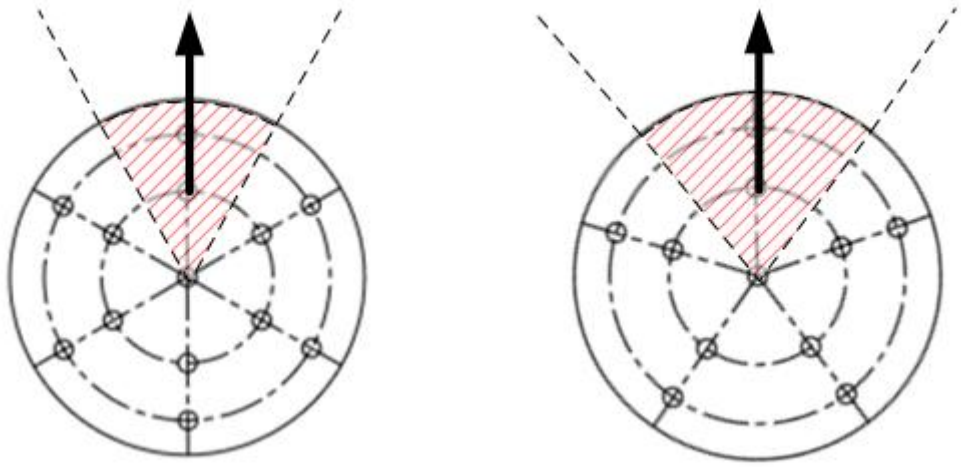

(a) Hexagonal disc (b) Pentagonal disc

Figure 18: Uniaxial loading of bolt array

Each individual bolt array is loaded uniaxially, as shown in Figure 18. For the most common design configurations, tension forces are usually the prevalent axial force in the structure (cf. Combination III in Table 3).

By inspection, a joint will always have a greater capacity against compressive failure than tensile failure[19], as the gross cross section of the material resists the load, whereas in tension only the net area of the material resists the load (as reductions must be made for bolt holes).

This means that even in cases where the largest magnitude axial force is compressive, if evidence can be provided to support that a joint will not fail under that magnitude of force in tension, then neither will it fail in compression. This simplifies our task of developing an equation to predict the failure load of the disc joints, as tensile failure alone can be conservatively considered.

5.3 Dimensional analysis

Massey [1998] states that complete solutions to engineering problems can seldom be obtained using analytical methods alone, and experiments are usually necessary to determine fully the way in which one variable depends on others. Dimensional analysis is a technique that can be applied to reduce the number of experiments required to obtain these relationships.

[19]This is assuming that instability (buckling) effects in compression may be ignored.

The first task in the process of dimensional analysis was to decide which variables may effect the solution and express them in terms of their dimensional formula. No quantity that may have affected the problem was overlooked, save for quantities that only had a indirect contribution[20]. The quantities considered were broken down into dimensional components (mass [M], length [L] and time [T]) in Table 4.

Table 4: Dimensional analysis: step 1

Quantity	Symbol	Dimensional forumula		
		[M]	[L]	[T]
Failure strength	f_u	1	-1	-2
Plate thickness	t	0	1	0
Hub radius	r	0	1	0
Axial force	F_{axial}	1	1	-2

The objective of dimensional analysis was to assemble the quantities into a smaller number of dimensionless groups. To achieve this, the variables were arranged in a way that removed their dependence on individual reference magnitudes, one after the other.

In this case, dependence on the mass dimension [M] was removed first, by dividing through by f_u, giving Table 5.

Table 5: Dimensional analysis: step 2

	[M]	[L]	[T]
f_u/f_u	1-1=0	-1-(-1)=0	-2-(-2)-0
t	0	1	0
r	0	1	0
F_{axial}/f_u	(1-1)=0	1-(-1)=2	(-2)-(-2)=0

As f_u/f_u gave unity, which is not a variable, it was eliminated. Dependence on the length dimension [L] was then removed by dividing through by r, giving Table 6.

Table 6: Dimensional analysis: step 3

	[M]	[L]	[T]
t/r	0	1-1=0	0
r/r	0	1-1=0	0
$F_{axial}/\left(f_u \times r^2\right)$	0	2-(1 × 2)=0	0

At this point, all dimensions had been eliminated from Table 6. r/r gives unity and was hence eliminated, leaving two reduced dimensionless groups:

$$\frac{F_{axial}}{f_u r^2} \quad and \quad \frac{t}{r} \tag{23}$$

[20]In Table 4, Young's modulus was neglected as this relates to the failure strength of the material. Similarly, temperature effects were ignored as these were material dependent.

In order to determine the relationship between these two groups, some experimental work was required.

5.4 Tension testing

5.4.1 Joint fabrication

Vigyan Ashram initially planned to send some sample joints for testing at Durham University; this was however ruled out due to expensive shipping costs. It was therefore necessary to design and fabricate some replica joints. Engineering drawings of the joints were subsequently drafted (see Appendix D), based upon the technical illustrations provided by Rolly [2007] and advice of Vigyan Ashram.

Durham University did not possess a press sufficiently powerful to create the bespoke joints from mild steel, hence a custom built press was instead used to fabricate joints from sheets of aluminium. Though not an ideal representation, the results would still be suitable for comparison between practical and computational models.

The joint fabrication was a labour intensive process, and hence only a limited number of discs were made. A total of six discs were made: two pairs of 1.5mm hexagonal and pentagonal discs and one pair of 2.0mm hexagonal and pentagonal discs.

5.4.2 Apparatus

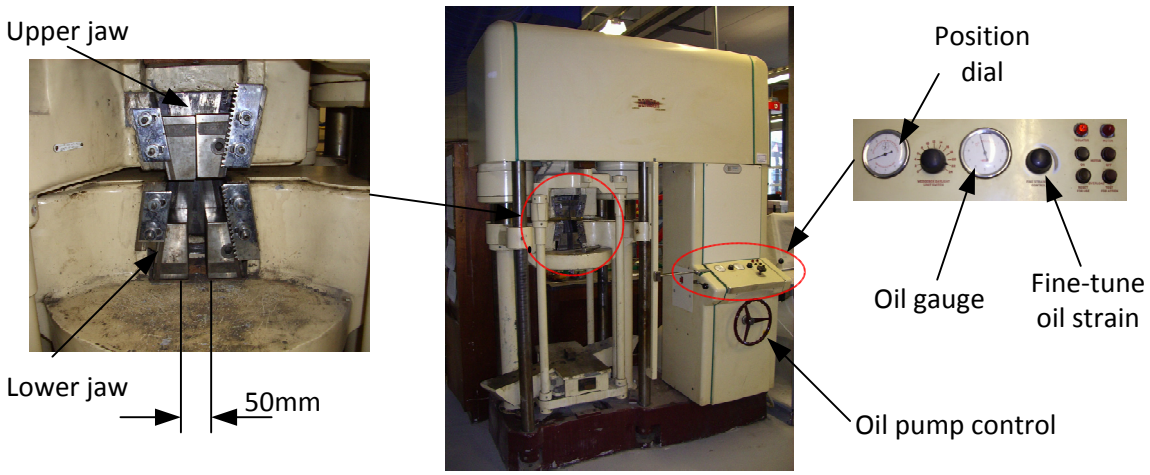

Figure 19: Denison loading machine

A Denison tension/compression loading machine was used for the tests (Figure 19). This machine was capable of applying a uniaxial tension force of up to 25kN, measuring force/displacment data electronically into a Windows based software package. At the time of use the machine was calibrated to a level complying with the United Kingdom Accreditation Standard (UKAS).

Finding a method of clamping the discs that would accurately represent the conditions to which the joint experiences in situ was problematic. A geodesic tensegrity network of the dome is three dimensional, whereas the Denison could only emulate one dimensional loading.

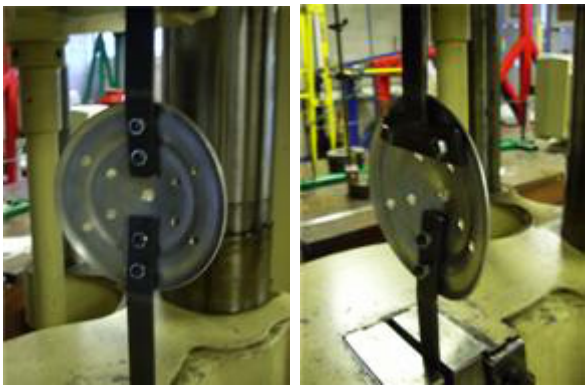

(a) Hexagonal rig (b) Pentagonal rig

Figure 20: Test rigs for joints

Several clamping methods were considered for the disc that would preserve the uniaxial tension case, but were hindered by the 50mm clearance between the teeth of the top and bottom clamps. It was decided to opt for a simple test rig using thumbscrews to attach the joint to predrilled (5mm thick) steel bars considerably stiffer than the test joint, as shown in Figure 20. This setup introduced a bending component into the tests, an undesirable effect, but was the most feasible option to allow experimentation to proceed.

5.4.3 Risk assessment

The experiment procedure was considered fairly low risk and only standard operating precautions were employed. As aluminium is a ductile metal, non-explosive failures were expected. The Risk Assessment and COSSH form for the experimental work may be found in Appendix F.

5.4.4 Method statement

The following operating procedure was used:

1. The Denison was switched on, and the oil feed activated to around half load, which began to separate the top and bottom clamps hydraulically. The oil feed rate was reduced to hold the Dension stationary when the top and bottom clamps were spaced approximately at the right height to fit in the test rig.

2. A joint was then selected for testing, and its thickness checked and noted at five approximately even spaces around its perimeter using a micrometer (accurate to

±0.005mm).

3. The joint was attached to the test rig using thumbscrew connections and clamped in the top and bottom jaws of the Denison.

4. The Denison datalogging software was loaded and the current position and registered force were set as datum values.

5. While continuing to hold the clamp closed with the winding key[21], the oil flow was increased so that the teeth continued to separate slowly. A load of approximately 0.2kN was applied before releasing the clamp.

6. The oil flow was continually adjusted to keep the rate of separation at approximately 0.025mm/s throughout the test to maintain a smooth loading curve.

7. When the disc failed, the test was stopped, and the positions of the top and bottom clamps were reset to an appropriate distance to repeat the above procedure for the next joint.

5.4.5 Results

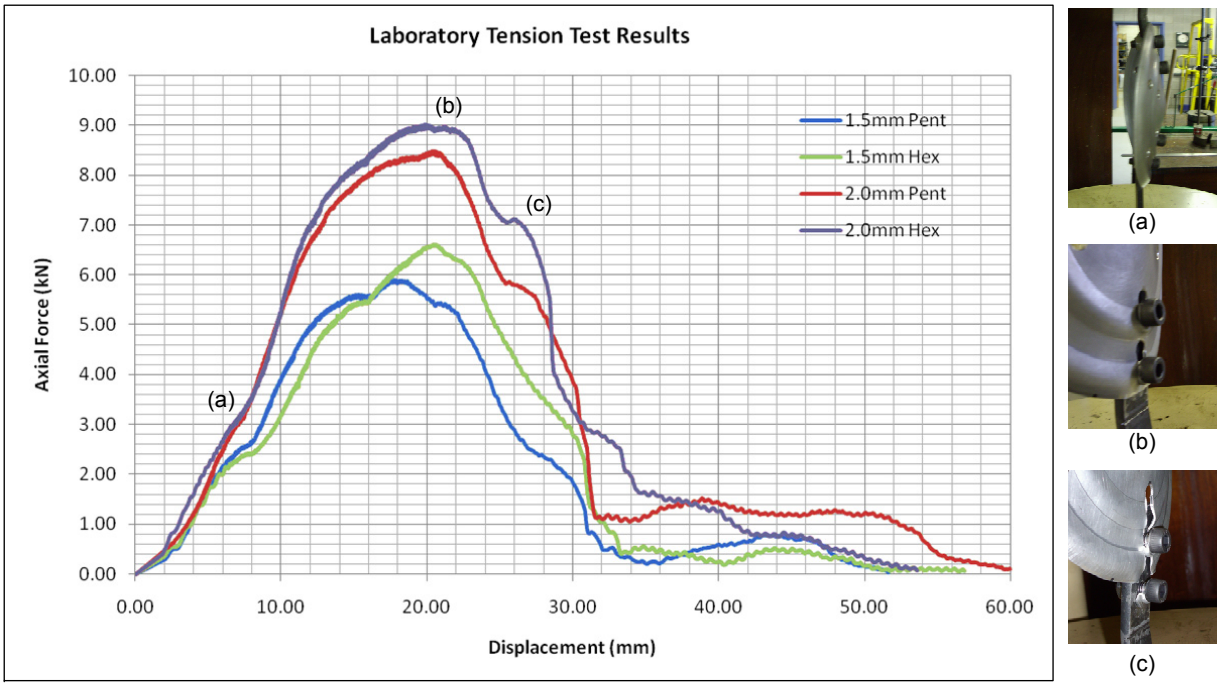

Figure 21: Tension test results

[21]This was because the clamps are held together by the friction of the teeth. When little or no load was applied, the teeth would slip free unless physically restrained from doing so.

The first pair of 1.5mm thick joints were tested as a trial run, in order to gain familiarity with the machine and experimental procedure before the full tests were run. The force-displacement plots for the remaining four joints are shown Figure 21.

5.4.6 Discussion

Several observations may be made about Figure 21. Each test plot begins approximately linearly, save for a kink at point (a), corresponding to the point where the disc deforms to align with the axial tension. Each disc reaches a peak capacity (b) after which the joint begins to tear in shear. Slight recoveries in strength were observed at point (c) as the joint crimps formed a necking region for torn material which temporarily impedes the shearing action.

Of particular interest was that the pentagonal joints in each case failed at a lower force than the hexagonal equivalents. This is counter intuitive as Figure 18 clearly shows that for a common load, the pentagonal bolt array will have a greater equivalent area to resist loading, so failure would be expected to occur hexagonal disc first.

This difference may be due to the less than ideal simplifications made for this test. In particular, the T-shaped clamping arrangement (Figure 20(b)) for the pentagonal disc was fairly far removed from the uniaxial tension case that was of interest and this may have adversely influenced its load capacity.

5.5 Stress analysis

A series of non-linear joint analyses were run using Strand to estimate the force at which joints would fail for various combinations of material parameters. Each test applied a series of incremental loads to the plate, calculating the resulting stresses and displacements in the material.

5.5.1 Model development

CAD models of the joints were created in Solidworks and imported to Strand. Problem symmetry was taken advantage of to reduce the analysis to the loaded area of a single bolt array (as shown by the hatched area of Figure 18).

Boundary conditions were prescribed along each of the two symmetry edges of the element, preventing any translation or rotation, save for radial slip. An incremental force was applied in the plane of the disc using a face pressure at each of the two bolt holes, representing the axial force transferred to the joint through the connection bolts.

The plates were meshed for analysis in two stages: a tet6 element surface mesh, followed by a tet10 brick mesh, both at a 3% mesh density. Before the investigation commenced, the mesh quality was checked using a convergence test. Three progressively finer meshes were run to calculate the planar displacement of an element at the center of

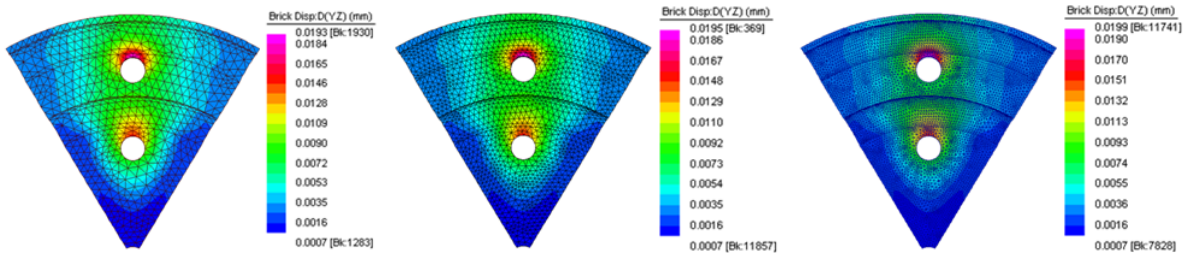

(a) 3% mesh (b) 2% mesh (c) 1% mesh

Figure 22: Mesh convergence

Table 7: Convergence test results

Mesh grade	Run time(s)	Displacement (mm)
3% mesh	6	0.0183190
2% mesh	18	0.0186015
1% mesh	718	0.0187712

the outer bolt hole (Figure 22). The results (Table 7) confirmed that the mesh quality was reasonable, as the results were clearly converging on a solution at ≈ 0.0188mm.

Three different plate thicknesses (1.5mm, 2.0mm and 3.0mm) and three different material properties (6082:T6 aluminium, S275 steel and S450 steel) were investigated. Results were repeated for both hexagonal and pentagonal material configurations, giving a total of 18 separate analyses. Ideally, the disc radius should also have been varied to fully investigate the dimensionless groups in Equation 23. However, a total of 54 analyses would have been required to investigate 3 radii variations, an unfeasible amount of work given the time frame of this project[22]. For duration of the computational work, the disc radius was fixed to 77.5mm.

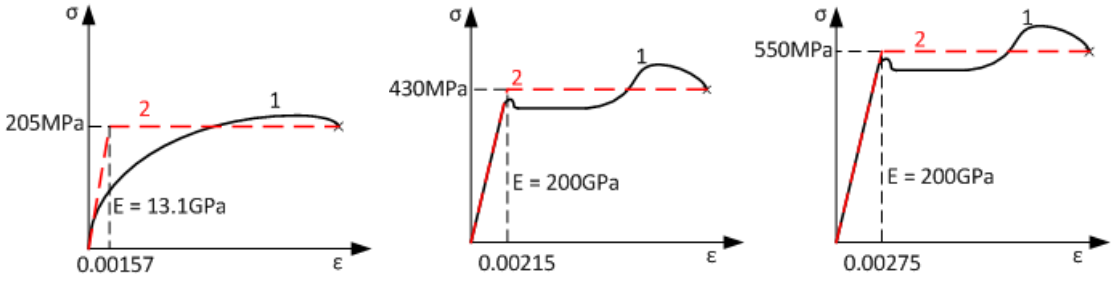

(a) Aluminium (AL6082) (b) Steel (S275) (c) Steel (S450)

Figure 23: Sketches of material stress-strain relationships

A linear static analysis could not be used to predict the failure load, as this assumes the material always behaves linear elastically. Non-linear analysis (Section 2.4.2) was instead

[22]The total required number of analyses to investigate a relationship increases to the power of the number of variables.

used, as this models the behaviour of the material as parts begin to deform plastically, until a limit is reached where deformation will continue indefinitely with no increase in applied force.

The model also assumed finite deformations, where the model progressively considers the deformed shape from the previous load increment. This is more representative of reality, but more computationally intensive than assuming infinitesimal strains and small displacements (where deformations are considered only relative to the original geometry).

Non-linear analysis required a stress-strain curve to be assigned to each material to inform Strand how the material would behave beyond yield. Material stress strain relatioships are often complex (see curve (1) in Figure 23), so to simplify the analysis, a perfectly plastic relationship was assumed, where ultimate failure was assumed at yield (curve (2) in Figure 23). This was a conservative assumption to make, as all the materials considered undergo plastic work hardening effects that improve capacity before ultimate failure.

5.5.2 Results

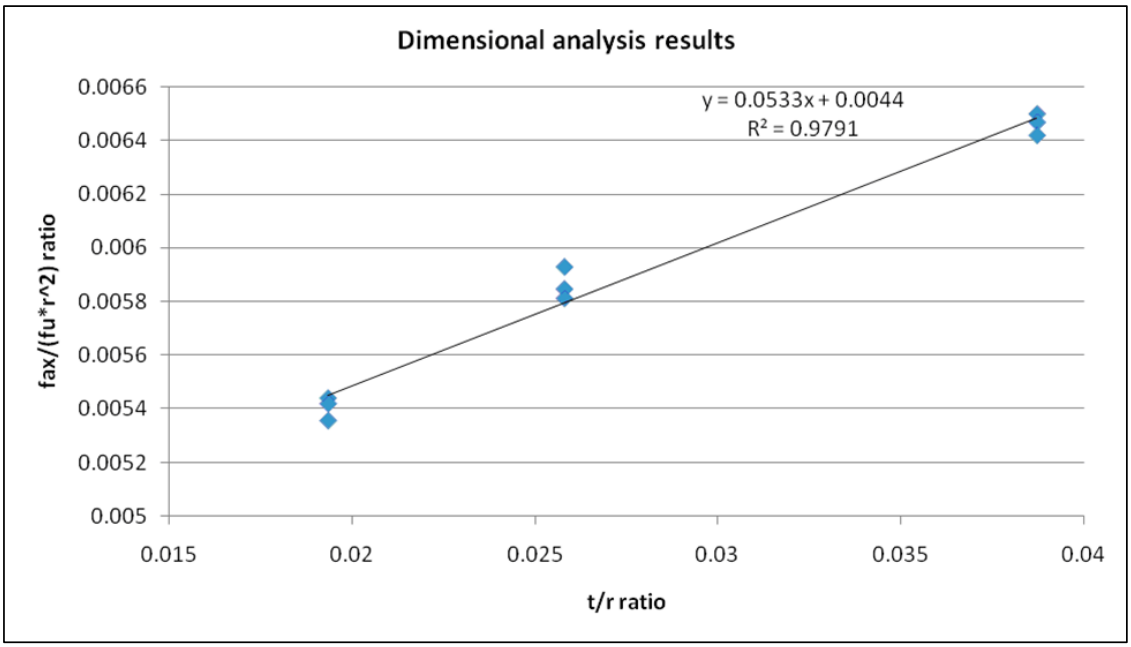

Figure 24: Plot of relationship between dimensionless variables

The force-displacement plots may be found in Appendix B. For each analysis, the axial force at which the displacement appeared to tend towards infinity (i.e. the ultimate load) was estimated from the graph (using the weaker 6-noded joint) and the dimensionless variable values from Equation 23 were calculated. The data used be found in Table 8 and the resulting graph from plotting the dimensionless groups is shown in Figure 24.

Table 8: Non-linear joint analysis results

Material	F_{axial}(kN)	t(mm)	f_u(MPa)	t/r	$F_{axial}/f_u r^2$
AL6082	6.7	1.5	205	0.0194	0.005441
AL6082	7.3	2.0	205	0.0258	0.005929
AL6082	8.0	3.0	205	0.0387	0.006497
S275	14.0	1.5	430	0.0194	0.005421
S275	15.1	2.0	430	0.0258	0.005847
S275	16.7	3.0	430	0.0387	0.006466
S450	17.7	1.5	550	0.0194	0.005421
S450	19.2	2.0	550	0.0258	0.005847
S450	21.2	3.0	550	0.0387	0.006466

5.5.3 Discussion

Figure 24 indicates some form of linear relationship may be established between the two variables. It is unreasonable to include the radius in the expression calculated, as its influence on the relationship was not rigorously tested. The linear polynomial of Figure 24 can therefore be simplified by fixing the considered radius size as a constant,

$$\frac{F_{axial}}{f_u \times 77.5^2} = 0.0533\frac{t}{(77.5)}0.0044 \ , \tag{24}$$

and rearranging,

$$F_{axial} = f_u \left(4.13t + 26.43\right) \ . \tag{25}$$

The force-displacement curves (Appendix B) indicated that for the theoretical stress analysis, the difference in capacity between hexagonal and pentagonal joint arrays was minimal. Intuitively, the pentagonal joint capacity was always the greater of the two in each test, in contrast to the practical test findings discussed in Section 5.4.6.

Table 9: Comparison of theoretical and practical joint capacities

Material	f_u (MPa)	t(mm)	r (mm)	Lab F_{axial}(kN)	Theoretical F_{axial}(kN)
AL6082	205	1.5	77.5	6.6	6.7
AL6082	205	2.0	77.5	9.0	7.1

As the pentagonal joint results were considered unreliable for the physical tests, the tensile failure values for the hexagonal value, taken from Figure 21, were compared to to the theoretical equivalents, calculated using Equation 25. The results shown in Table 9, though not comprehensive, indicate that for low joint thicknesses the theory accurately predicts the failure force, while for greater thicknesses it provides a 20% underestimation of their capacity.

There are a number of reasons that the theoretical estimations become overly conservative.

A possible cause is that isotropic work hardening effects were neglected in the theoretical model (see Figure 23), and this contribution became more pronounced as the thickness of the joint increased.

A trade-off between computational efficiency and accuracy had to be made, and it is possible that the FE mesh was not fine enough to obtain good results. Additionally, the boundary conditions assumed in the model represented a worst case, and in reality limited displacements take place at the assumed boundaries of the disc segement modelled.

A final possible reason for the reserve strength of the joint is that the loaded segment area was conservatively assumed. When the joint as a whole is loaded, it reaches a state of equilibrium. As not all the loads on the joint may be of the same magnitude, it logically follows that larger bolt arrays may be supported by a larger area of the joint than that assumed, and therefore have a greater capacity of resistance.

6 Spreadsheet development

This section of the report describes how the FEA based package for analysing geodesic domes works, with reference made to the theory of Section 3. The features that make the layout user friendly and accessible, as well as limitations of the package, are also discussed.

6.1 Package structure

The package was broken down into three Excel files, as a single spreadsheet became unwieldy to run due to the large amount of data being processed. These files guide the user through the stages of performing a dome analysis and design. First, the user defines a geometry and loading case on the structure in "FEA_Input". The spreadsheet subsequently calculates the force vector which is read into the second spreadsheet "FEA_Solver", where the structure stiffness matrix is formed. Equation 12 is then solved for the structure displacements. The final spreadsheet, "FEA_Output", post-processes the displacement results to give member forces in the structure. The worst case force produced is utilised in a series of calculations that allow the user to optimise the structure to carry the load and make savings on materials.

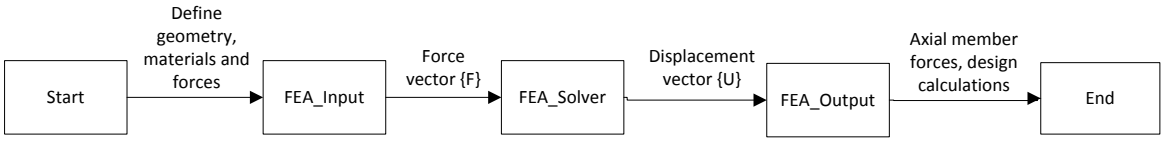

Figure 25: Flow chart of design process

6.2 FEA_Input

FEA_Input is the spreadsheet in which the user defines all the parameters of a particular dome - geometry, materials, loads and partial safety factors. The main output of the spreadsheet is the force vector.

The spreadsheet consists of five worksheets, described below.

- **Summary**: this is the only worksheet in the FEA_Input file requiring user interaction. All the variables are defined here, and the various worksheets tabs link to these parameters to calculate forces. The force vector is calculated based on the summation of various factored loads.
- **Graphs**: the level of soil applied to the structure above the base of the foundations is calculated and represented graphically on this worksheet. Additionally, this page shows which portion of the dome is considered loaded.
- **Soil**: the nodal forces in the structure due to soil loading are found using Rankine's theory for earth retaining structures as described in Section 4.3.3. Various soil types may be selected from, imposing different parameters on the calculations. The user can also specify the depth and area of the dome that is loaded.
- **Wind**: this worksheet calculates the worst case effect of a wind pressure acting on one face of the structure, based on a user-defined wind load (see Section 4.3.4 for details).
- **SW & Imposed**: the nodal forces due to the self weight of the structure and due to any specified imposed loading are calculated in this worksheet. The methodology of this was previously discussed in Section 4.3.5.

6.3 FEA_Solver

The FEA_Solver spreadsheet emulates the stiffness method discussed in Section 3.1 to form Equation 12. A Gaussian elimination method is then used to solve for the displacement vector $\{U\}$. The solver spreadsheet runs automatically when opened, with no user input required.

6.3.1 Stiffness matrix assembly

The spreadsheet first reads in the force vector and specified parameters from FEA_Input and uses the information about the geometry to scale the coordinates in the "nodal coordinates" worksheet. This in turn is used to calculate the total length L of each member

	A	B	C	D	E	F	G
1							
2							
3	E =	2.00E+11	N/m²				
4	A =	1.57E-04	m²				
5							
6							
7	Element	Node	Node	L_x	L_y	L_z	L (m)
8		(end 1)	(end 2)	(x_2-x_1)	(y_2-y_1)	(z_2-z_1)	
9	1	1	2	0.0000	1.0464	-0.1853	1.0627
10	2	2	3	0.9952	-0.7230	0.0000	1.2301
11	3	3	1	-0.9952	-0.3234	0.1853	1.0627

Figure 26: Calculation of project member lengths

and the axis projected lengths L_x, L_y, L_z (as shown in Figure 26), using predetermined information about how elements and nodes link together in the structure[23].

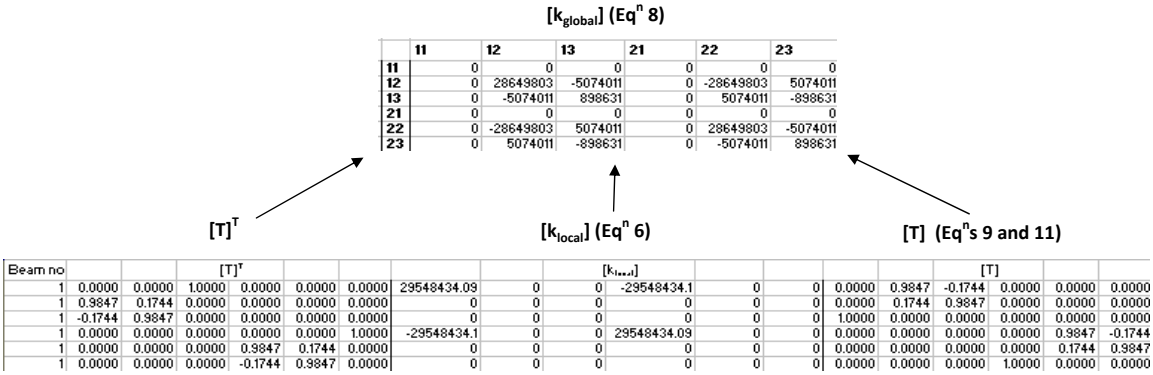

	11	12	13	21	22	23
11	0	0	0	0	0	0
12	0	28649803	-5074011	0	-28649803	5074011
13	0	-5074011	898631	0	5074011	-898631
21	0	0	0	0	0	0
22	0	-28649803	5074011	0	28649803	-5074011
23	0	5074011	-898631	0	-5074011	898631

Beam no	[T]^T						[k_local]						[T]					
1	0.0000	0.0000	1.0000	0.0000	0.0000	0.0000	29548434.09	0	0	-29548434.1	0	0	0.0000	0.9847	-0.1744	0.0000	0.0000	0.0000
1	0.9847	0.1744	0.0000	0.0000	0.0000	0.0000	0	0	0	0	0	0	0.0000	0.1744	0.9847	0.0000	0.0000	0.0000
1	-0.1744	0.9847	0.0000	0.0000	0.0000	0.0000	0	0	0	0	0	0	1.0000	0.0000	0.0000	0.0000	0.0000	0.0000
1	0.0000	0.0000	0.0000	0.0000	0.0000	1.0000	-29548434.1	0	0	29548434.09	0	0	0.0000	0.0000	0.0000	0.0000	0.9847	-0.1744
1	0.0000	0.0000	0.0000	0.9847	0.1744	0.0000	0	0	0	0	0	0	0.0000	0.0000	0.0000	0.0000	0.1744	0.9847
1	0.0000	0.0000	0.0000	-0.1744	0.9847	0.0000	0	0	0	0	0	0	0.0000	0.0000	0.0000	1.0000	0.0000	0.0000

Figure 27: Assembly of the global stiffness matrix

Each local element stiffness matrix $[k_{local}]$ is calculated using Equation 6. Using the projected member lengths, $[R_0]$ and resultantly $[T]$ are found for each element using Equations 11 and 9 respectively, which may be transposed to find $[T]^T$. Finally, Equation 8 is used to determine the global element stiffness matrix (see Figure 27).

The numbering scheme used for degrees of freedom may appear abstract at first, but the system was chosen to add clarity to which degree of freedom was under scrutiny - the last number is always "1", "2" or "3", referring to whether it was an X, Y or Z directional DOF in the global coordinate system. The remainder of the number (disregarding the last unit) describes which node the degree of freedom belongs to. For example, "312" would refer to node 31's Y directional DOF.

In order to assemble the full structure stiffness matrix from the 165 global element stiffness matrices without resorting to a programming script, several intermediate stages were used in Excel to get the data in a form that allows the summation of cells with common values, as described below.

[23]The knowledge of how the elements link up was a feature built-in to the spreadsheet, based on the element and node numbering scheme used by Strand7.

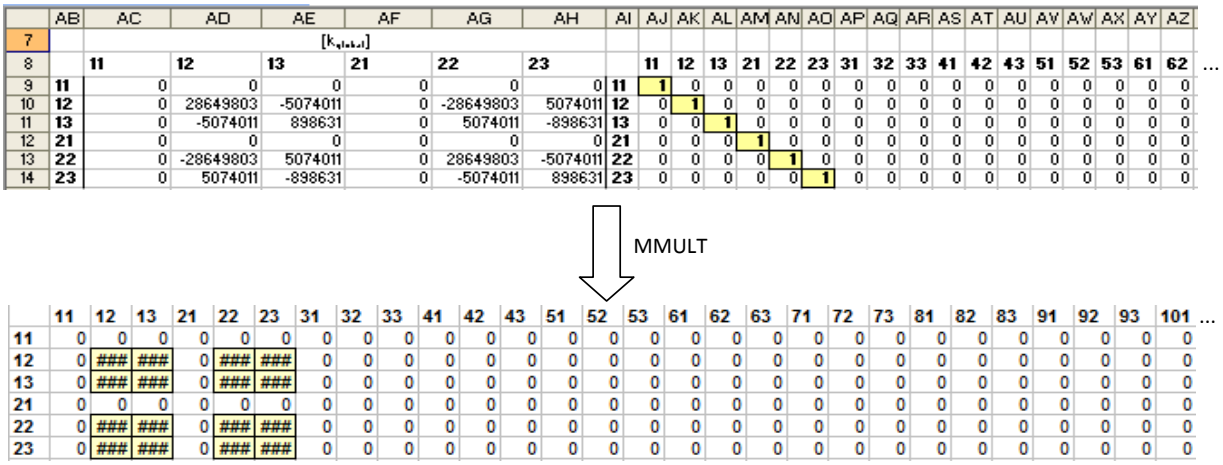

Figure 28: Intermediate matrix assembly step

1. A 6×183 Boolean matrix[24] [B] was created for each element. This matrix was labelled such that only the rows with DOF associated with the local stiffness matrix were considered, whereas the full list of 183 degrees of freedom were included for the columns. Excel checked each cell's row and column reference, producing a zero if they do not match, and a one if they do (Figure 28).

2. For each element, the global stiffness matrix and the Boolean matrix were then multiplied together using Excel's built in matrix multiplication function "MMULT". This produces a partly assembled version of the structure stiffness matrix, which shall be henceforth referred to as an intermediate $[C]$ matrix. This can be thought of as fully assembled in terms of columns but not rows (Figure 28),

$$[C] = [k_{global}][B] \; . \tag{26}$$

3. Once a $[C]$ matrix was produced for each element, it was possible to sum all the matching rows in the assembly to complete the full 183×183 structure stiffness matrix. An Excel function known as "SUMPRODUCT" was used to achieve this: for each cell in the 183×183 structure stiffness matrix, the calculation seeks the row and column DOF reference of the cell and then looked for each corresponding row and column match in the intermediate matrices. It then summed together the cell values for all the matches and outputs the result in the structure stiffness matrix.

Figure 29 shows an example of the method for a simple set of matrices. For instance, if the value of the assembled structure stiffness matrix circled in red was of interest, the SUMPRODUCT function would seek its reference position (2,2) and look in the above

[24] A Boolean matrix is a matrix with entries from the Boolean domain $B = \{0, 1\}$. Such a matrix can be used to represent a binary relation between a pair of finite sets [Flegg, 1965].

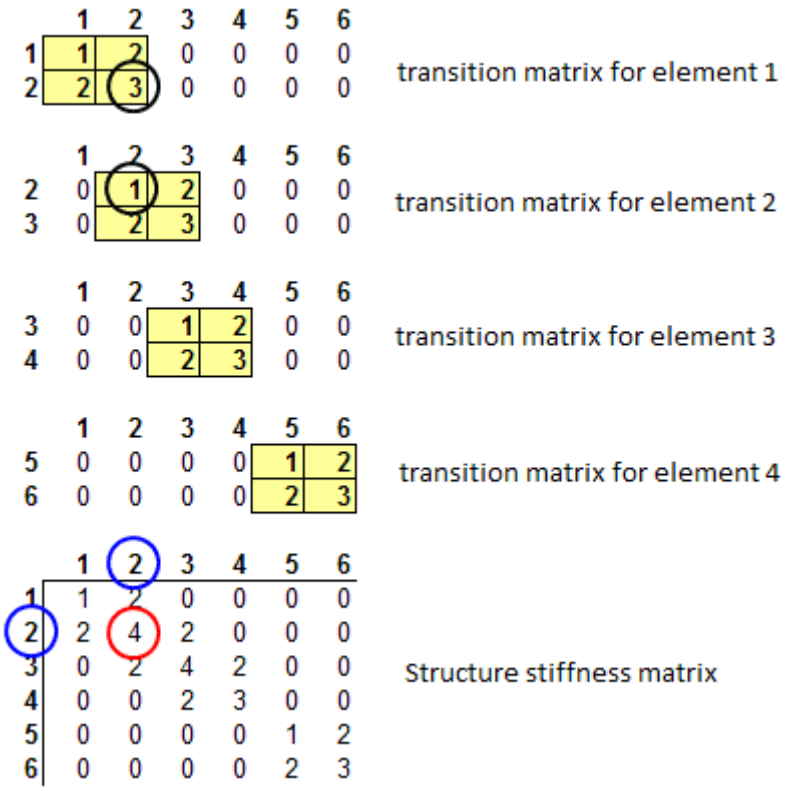

Figure 29: Structure stiffness matrix assembly using SUMPRODUCT

transition matrices for the same reference numbers. In this case, it would find two matches, circled black. The matching cells are summed to get the final value which is output in the assembled structure stiffness matrix. The same principles apply for the calculation of each stiffness value in the structure stiffness matrix.

6.3.2 Solver

At this point, the spreadsheet has fully defined the force vector $\{F\}$ and structure stiffness matrix $[K]$ in Equation 12. In order to solve the system, Excel uses a built-in macro written in Visual Basic for Applications (VBA) to perform Gaussian elimination. This solver method was chosen as it is popular and well documented, making it easier for someone wishing to learn the mechanics to follow (see Section 3.2).

This code was adapted from one presented in Billo [2007], operating as a user defined array function[25] in the form: *GaussElim(coeff_matrix, const_vector)*, where coeff_matrix is set to equal the cell reference area of the structure stiffness matrix, and const_vector is set as the cell reference area of the force vector; both having been first reduced by applying the perimeter ring boundary conditions.

[25] An array function is a special method of calculation employed when working with arrays, matrices and vectors. Rather than applying one formula to one cell, a formula is applied to an array of cells. For more information, see Pearson [2008].

6.4 FEA_Output

The main purpose of the FEA_Output spreadsheet is to determine the internal axial member forces by post processing the results of the structure stiffness method, and to allow the user to tailor the fabrication details of the dome so that a safe and economical design is produced.

6.4.1 Postprocessing

								(Eq^n 15)	$u_2 - u_1$	(Eq^n 3)	(Eq^n 4)	(Eq^n 2)
Elem no	DOF	U (mm)		[R_0]			u_{local} (mm)	Δu_x (mm)	ε	σ (MPa)	F_{axial} (kN)	
1	11	0.00	0.0000	0.9847	-0.1744		0.3099					
1	12	0.04	0.0000	0.1744	0.9847		-1.5173					
1	13	-1.55	1.0000	0.0000	0.0000		0.0002	-0.0858	-0.000081	-16.15	-2.5	
1	21	0.00	0.0000	0.9847	-0.1744		0.2240					
1	22	-0.02	0.0000	0.1744	0.9847		-1.3746					
1	23	-1.39	1.0000	0.0000	0.0000		0.0013					

Figure 30: Calculation of member axial forces

The first step taken by Excel is to import the displacement vector previously calculated in FEA_Solver. Information about the member lengths and properties are also read into the worksheet. The displacements are sorted by DOF for each element, and the transformation matrix (Equation 11) is applied in reverse for each node to get the displacements back in terms of the elements' local coordinate system. Note that the spreadsheet uses $[R_0]$ to transform each node's 3 degrees of freedom, rather than applying the full transformation matrix to the full force vector as described in Equation 9. The methods are entirely equivalent, but the chosen approach is slightly more compact and therefore a better method of displaying the information.

The local x' (Figure 8) axis displacements are subtracted from one another, giving the change in length of the element due to the applied external forces on the structure. The strain in each member is calculated using Equation 3, and, by virtue of Hooke's law, the stress can be found using Equation 4. Finally, the axial force in each element is found using Equation 2 (see Figure 30).

6.4.2 Calculations

The calculation worksheet was designed to produce a comprehensive document summarising any analysis and design case. The layout was thereby set out in a printer friendly format, so that pdf or paper based printouts could be made for permanent record. An example calculation print out may be found in Appendix E.

The worksheet was designed, where possible, to the guidelines of Eurocode 3 [BSI, 2007]. The ultimate design load of the structure was set as largest magnitude axial force

calculated in the elements during post processing[26]. The spreadsheet makes checks for safety for the Ultimate Limit State (ULS) and Serviceability Limit State (SLS).

The following four design checks were considered:

- **Joint shearing failure (ULS)**: this check used the empirical relationship developed in Section 5 to estimate joint capacity. Equation 25 is additionally factored by a material constant to represent variable material strengths in steel.
- **Bolt connections (ULS)**: the bolts were checked using guidelines laid out for steel bolted connections in EC3, Section 3: Connections made with bolts, rivets or pins. Checks were made for both shear and bearing resistance of the bolts.
- **Angle section (ULS)**: this checked the capacity of the equal angle truss elements used by Vigyan Ashram against failure in tension at their smallest net cross-section, i.e. where holes are drilled for the connections, using the guidelines in EC3-80, Section 3.10.3. Bending moment checks for the section were not required for the reasons discussed in Section 2.3.3.
- **Deflection limit (SLS)**: this check was introduced to avoid severe deformations of the structure that would impede its appearance or functionality under working loads. The deflection limit was set to $L/360$, which the Eurocodes presented as the most suitable limiting value for a member clad in a brittle material subject to cracking (EC3-59, Section 7.2).

The worksheet also calculates relevant fabrication details, such as the number of joints and different member lengths required to assemble the dome and utilises conditional picture formatting to produce subdivision assembly diagrams for the dome (from Landry [2002]) depending on which configuration is selected. It should be noted that while the fabrication and assembly details can be calculated for many different dome configurations, the FE solver method currently only considers the V3 5/8ths dome (see Section 4.4). The expanded version of the fabrication details were created in anticipation that further work may be carried out on the package to expand its analysis capability to any type of dome. At present, the worksheet has warning features built in to inform the user if they attempt a design mismatched from the analysis capabilities.

6.5 Discussion

Before the accuracy of the spreadsheet based analysis is compared to the benchmark results set by Strand7, it is worthwhile discussing some of the features that make the spreadsheet package user-friendly and well suited to the aims of this project.

[26]The reason this assumption could be made without regard to whether it is tensile or compressive was covered in Section 5.2.

Firstly, the step-by-step layout of the spreadsheet (Fig. 25) leads the user through distinct stages of modelling, analysis and design. By keeping to this format, the layout of the spreadsheets was orientated towards explaining the purpose of each step.

While it is entirely possible to perform an analysis using this package without in-depth understanding of the inner workings of the calculations, these were left visible and accessible to the users interested in learning how the analysis works. To aid with understanding the FE method, a user-guide was produced to accompany the package, explaining the basis of the FE method and how the spreadsheet emulates it. Black box steps were avoided wherever possible in the spreadsheets. For example, the structure stiffness matrix may have been more efficiently assembled using a VBA macro, but the step-by-step approach implemented in the spreadsheet was felt to be more suitable, as it demonstrates the process with greater clarity. The only exception to this was Gaussian elimination, which had to be performed as a Visual Basic script due to the looping nature of solving a problem using this method.

Use was made of Excel based features such as conditional formatting to highlight cells of interest (e.g. passed or failed calculation checks) or to add conditional warnings if the user attempts something inadvisable (e.g. spacing bolts closer than the recommended limit). Additional advice was provided to the user using Excel's cell commenting feature, where hovering over a commented cell brings up an information box with additional dialogue explaining its function.

Table 10: Spreadsheet based FEA results

Case	Max. Axial Forces (kN)		Max. Disp (mm)	% Relative error
	Tensile	Compressive	u_e	(cf. Table 3)
Case I	4.2329	3.0366	-0.8960 (Z)	9.998×10^{-5}
Case II	10.2997	69.7237	-6.8789 (Z)	2.907×10^{-5}
Case III	33.3654	102.4467	7.8202 (X)	3.836×10^{-5}
Case IV	1.0610	1.1811	0.2248 (X)	0.000×10^{-5}
Case V	2.1607	1.5500	-0.4570 (Z)	21.188×10^{-5}
Combination I	21.8353	99.5682	-9.9605 (Z)	4.016×10^{-5}
Combination II	39.6277	143.9114	-13.0222 (Y)	0.768×10^{-5}
Combination III	7.7372	5.9747	-1.5108 (Z)	6.619×10^{-5}

The results of the spreadsheet FE method are shown in Table 10. The boundary conditions, forces and design assumptions made were identical to the case described in Section 4.5. The relative error for each load case was found by normalising the maximum Excel displacement u_e by the maximum Strand7 displacement u_s (from Table 3) and expressing it as a percentage:

$$error = \left(1 - \frac{u_e}{u_s}\right) \times 100 \, . \tag{27}$$

For each load case, the relative error between Strand7 and Excel was found to be negligibly small, indicating that the spreadsheet based FE method accurately imitates the commercial package. The computation time to reach a solution was significantly longer in Excel (typically 30-60s in the spreadsheet cf. to 3s in Strand), as may be expected, but as the point of the exercise was not one of solver efficiency, this fact is perhaps unimportant.

7 Conclusions

Returning to the objectives defined in the project plan, it is possible to assess how completely the project objectives have been met. The main goal of this project worked towards producing a Microsoft Excel based structural analysis method, to give Vigyan Ashram the in-house capability to perform structural analysis. This has been successfully met, with a spreadsheet based system that reproduces the results of an considerably more expensive commercial finite element package using the structure stiffness method. A wide variety of different load types and geometries can be applied to the dome, making the package a versatile analysis tool.

The system has been designed for ease of use, even for someone with a minimal understanding of the method, while also leaving the mechanics of the method clear for those who wish to learn it.

The objective to produce fabrication and design information has also been successfully integrated into the package, leading the user from the stage of forming and analysing a dome model through to using the results of the analysis to design safe joint connections.

A linear relationship was found between material properties and estimated failure strength of the dome's joints. Though this appeared to correlate well, time limitations prevented a thorough testing of the influence of disc radius as a variable.

The physical tension tests performed were good for comparative, empirical studies, and the results confirmed the theoretical relationship developed was a good match. However, the accuracy of the values was questionable as they did not reproduce real conditions, and more work would ideally need to be carried out to confirm the validity of the relationship.

The results of the Strand7 analysis were indicative of the problem in the Water Bank project using subterranean domes; very large compression forces became prevalent in the structure, especially in cases of asymmetric loading.

7.1 Further work recommendations

- Expansion of the spreadsheet method to consider more dome configurations. Currently the analysis focuses on the most common configuration (V3 5/8ths), but with work this could be expanded, offering more flexibility in terms of fabrication and

the size of structure that can be produced[27].

- In depth investigation of the Water Bank project subterranean loading case. Though the analysis and designs tools discussed in this dissertation will produce a safe design for a subterranean dome, conservative assumptions were made to simplify the loading and the capacity of the structure that may need to be reviewed for this special case. For example, the contribution of any passive resistance in the soil was neglected and the testing of the joints focused on tensile rather than compressive failure.

- Work on improving the efficiency of the spreadsheet solver. For higher order problems, it may be necessary to investigate the implementation of node ordering algorithms to minimise matrix bandwidth [Cuthill and McKee, 1969].

- Investigation into the design of the dome to improve load bearing capacity. For example, discs were the only joint considered as they are the design which Vigyan Ashram currently use and are set up to manufacture. Alternative joint designs may prove to be cheaper, easier to fabricate or stronger.

- The modification of the spreadsheet analysis method to work on a freeware package, such as OpenOffice[28], so that the software cost associated with the program is eliminated entirely.

[27] As member lengths for lower frequency domes will fail in buckling if particularly large radius domes are planned; this limits the size of dome that can be achieved using a V3 dome frequency.

[28] http://www.openoffice.org/

References

N.M. Bhandari, P. Krishna, and K. Kumar. IS875: Wind loads on buildings and structures. [Last Accessed: 28th February 2009], 1987. URL http://www.iitk.ac.in/nicee/IITK-GSDMA/W02.pdf.

N.M. Bhandari, P. Krishna, and K. Kumar. Wind storms, damage and guidelines for mitigative measures. [Last Accessed: 28th February 2009], 2003. URL http://www.iitk.ac.in/nicee/IITK-GSDMA/W03.pdf.

E. J. Billo. *Excel for Scientists and Engineers – Numerical Methods*. John Wiley and Sons, 2007.

BSI. *Structural Eurocodes*. MFK Group, second edition, 2007.

Robert William Burkhardt. A practical guide to tensegrity design. [Last Accessed: 19th February 2009], 2007. URL http://bobwb.tripod.com/tenseg/book/revisions.html.

R.C. Coates, M.G Coutie, and F.K. Kong. *Structural Analysis*. Chapman and Hall, third edition, 1988.

Fiona Cobb. *Structural Engineer's Pocket Book*. Blackwell House, 2007.

R. F. Craig. *Craig's Soil Mechanics*. Spon Press, seventh edition, 2004.

E. Cuthill and J. McKee. Reducing the bandwidth of sparse symmetric matrices. *In Proc. 24th Nat. Conf. ACM*, pages 157–172, 1969.

T. Davis. Gedoesic domes. [Last Accessed: 18th January 2009], 2007. URL http://www.geometer.org/mathcircles/geodesic.pdf.

D. J. Dowrick. *Earthquake Resistant Design - A manual for Engineers and Architects*. John Wiley and Sons, Ltd., 1978.

H. Graham Flegg. *Boolean Algebra and its application*. Blackie, University of California, 1965.

J. P. Hartog. *Understanding ferrocement construction*. VITA, Arlington, Virginia, 1984.

Indian Express. No geodesic structures for quake site. Newspaper Article, October 13th 1993.

Infobase. Natural hazard map of india. [Last Accessed: 1st March 2009], 2000. URL http://www.mapsofindia.com/maps/india/natural-hazard.htm.

S. Kalbag. Vigyan Ashram: Rural development education system. [Last Accessed: 18th January 2009], 2004. URL `http://www.vigyanashram.com/`.

M. Kardysz, J. Rebielak, and R. Tarczewski. Loading behaviour of some types of tension-strut domes. *Space Structures 5*, 2:1209–1218, 2002.

H. Kenner. *Geodesic math and how to use it.* University of California Press, second edition, 2003.

K. Knebel, J. Sanchez-Alvarez, and S. Zimmermann. The structural making of the Eden domes. *Space Structures 5*, 1:245–254, 2002.

Erwin Kreyszig. *Advanced Engineering Mathematics.* John Wiley and Sons, Inc., ninth edition, 2006.

Tara Landry. Dome formulas. [Last Accessed: 8th March 2009], 2002. URL `http://www.desertdomes.com/formula.html`.

Z. S. Makowski. Steel space structures. *Building with Steel*, 11:2–10, 1972.

Z. S. Makowski. *Steel Space Structures.* Michael Joseph, Battersea College of Technology, London, UK, 1965.

Z. S. Makowski. Braced domes. *Building Specification October Edition*, pages 37–46, 1979.

Z. S. Makowski. *Analysis, Design and Construction of Braced Domes.* Granada, University of Surrey, UK, 1984.

MapXL. Annual temperature map of india. [Last Accessed: 27th February 2009], 2006. URL `http://www.mapxl.com/indiamaps/annual-temperature.html`.

Bernard Massey. *Mechanics of Fluids.* Spon Press, seventh edition, 1998.

J.L. Meek and S. Loganathan. Large displacement analysis of space frame structures. *Computer methods in applied mechanics and engineering*, 72:57–75, 1989.

W. Morgan. *The Elements of Structure.* Pitman, University of Auckland, New Zealand, second edition, 1981.

R. Motro. Review of the development of geodesic domes (ed. Makowski). *Analysis, Design and Construction of Braced Domes*, pages 387–412, 1984.

P. Mullord. Introduction to the analysis of braced domes (ed. Makowski). *Analysis, Design and Construction of Braced Domes*, pages 86–95, 1984.

P.D. Pakandam and B. Sarshar. Comparison of the behaviour of 3 types of braced dome. *Space Structures 4*, 1:359–368, 1993.

C. Pearson. Array formulas. [Last Accessed: 23rd February 2009], 2008. URL `http://www.cpearson.com/excel/ArrayFormulas.aspx`.

V. Quintas and J. M. Avila. An analysis of braced domes. *Space Structures 4*, 1:265–274, 1993.

G. Ranjan and A.S.R Rao. *Basic and Applied Soil Mechanics*. New Age International Publishers, second edition, 2000.

D. L. Richter. Space structures development from early concept to temcor geodesic domes. *2nd International Space Structures Conference*, pages 534–549, 1975.

Horst Friedrich Rolly. *Earthquake Disaster Management*. Peter Lang, Frankfurt, Germany, 2007.

J.S. Sanchez-Alvarez. Introduction to the analysis of braced domes (ed. Makowski). *Analysis, Design and Construction of Braced Domes*, pages 175–244, 1984.

A.V. Shroff and D.L. Shah. *Soil Mechanics and Geotechnical Engineering*. Taylor and Francis, 2003.

K. A. Stroud. *Engineering Mathematics*. Palgrave Macmillan, fifth edition, 2001.

Kian Teh and Laurie Morgan. The application of excel in teaching finite element analysis to final year engineering students. Proceedings of the 2005 ASEE/A aeE 4th Global Colloquium on Engineering Education, 2005.

Jon Trevelyan. Level 3 stress analysis. [Course lecture notes], 2007.

Thomas T. K. Zung. *Buckminster Fuller: Anthology for the New Millennium*. St. Martin's Press, New York, USA, 2001.

A Project Gantt chart

Task Name	Duration	Start	Finish
Project Start	**0 days**	**Thu 25/09/08**	**Thu 25/09/08**
Initial Research and Planning	**83 days**	**Thu 25/09/08**	**Mon 19/01/09**
Prelminary Research	10 days	Thu 25/09/08	Wed 08/10/08
Ongoing Research	73 days	Thu 09/10/08	Mon 19/01/09
Modelling and Analysis	73 days	Thu 09/10/08	Mon 19/01/09
Risk Assessment	2 days	Fri 24/10/08	Mon 27/10/08
Risk Assessment Deadline	0 days	Mon 27/10/08	Mon 27/10/08
Project Plan	6 days	Fri 24/10/08	Fri 31/10/08
Project Plan Deadline	0 days	Fri 31/10/08	Fri 31/10/08
Joint design & Technical Drawings	29 days	Fri 31/10/08	Wed 10/12/08
Literary Review Writeup	29 days	Wed 10/12/08	Mon 19/01/09
Literary Review Deadline	**0 days**	**Mon 19/01/09**	**Mon 19/01/09**
Data Collection and Analysis	**103 days**	**Mon 01/12/08**	**Wed 22/04/09**
Experimental Work	20 days	Mon 19/01/09	Fri 13/02/09
Draft Report	75 days	Mon 01/12/08	Fri 13/03/09
Draft Report Deadline	**0 days**	**Fri 13/03/09**	**Fri 13/03/09**
Revision of Report	24 days	Fri 20/03/09	Wed 22/04/09
Project Conclusions	**18 days**	**Wed 22/04/09**	**Fri 15/05/09**
Final Submission Preparation	6 days	Wed 22/04/09	Wed 29/04/09
Final Submission	**0 days**	**Wed 29/04/09**	**Wed 29/04/09**
Poster Preparation	6 days	Fri 24/04/09	Fri 01/05/09
Oral Exam Preperation	11 days	Fri 01/05/09	Fri 15/05/09
Oral Exam	0 days	Fri 15/05/09	Fri 15/05/09
Project End	**0 days**	**Fri 15/05/09**	**Fri 15/05/09**

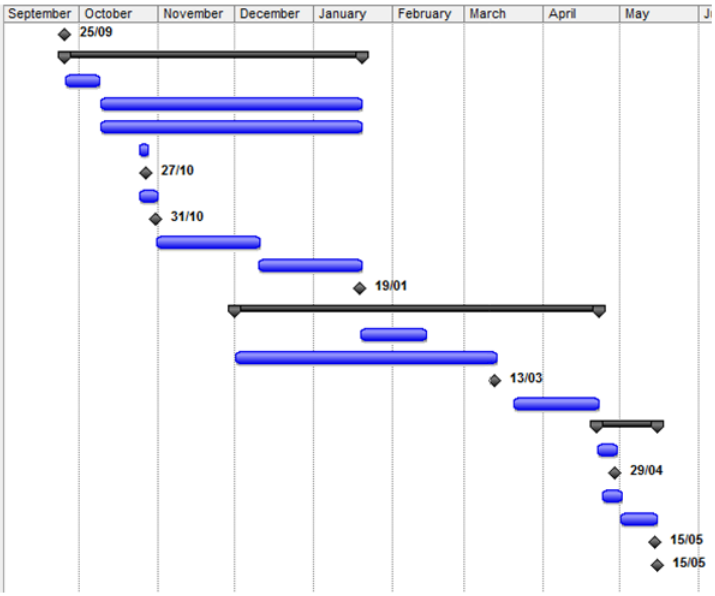

Figure 31: Project Gantt chart

B Joint force-displacement curves

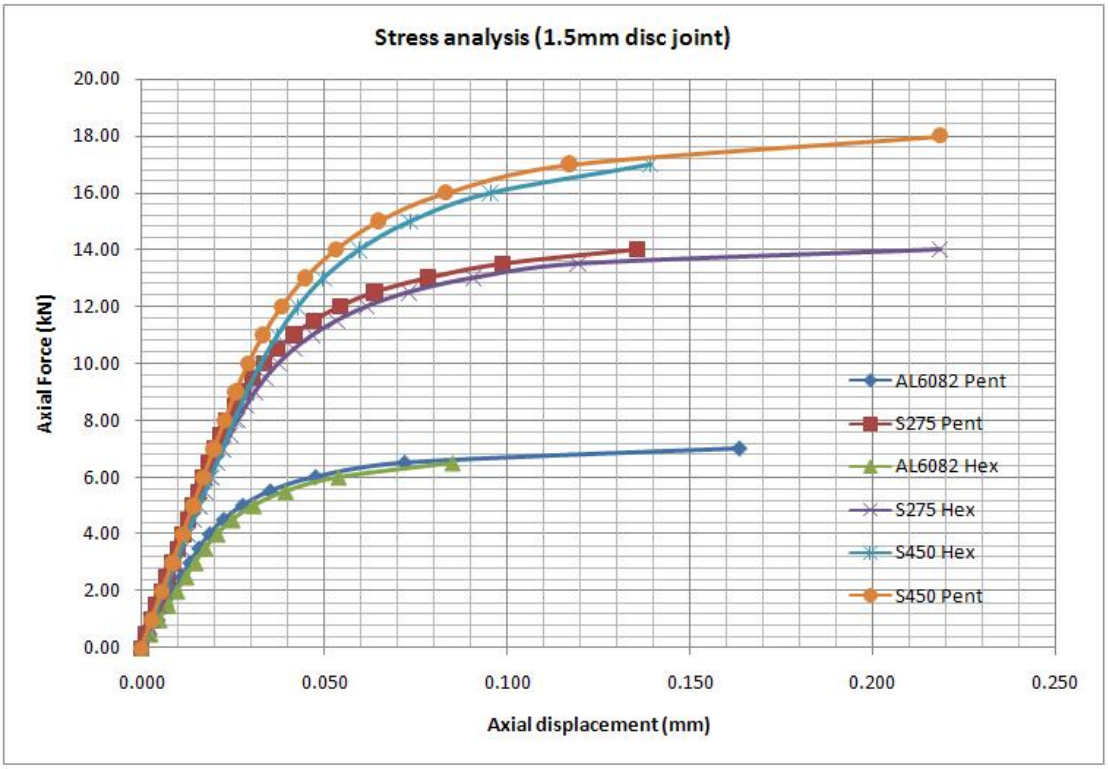

Figure 32: Stress analysis force-displacement plot for 1.5mm disc

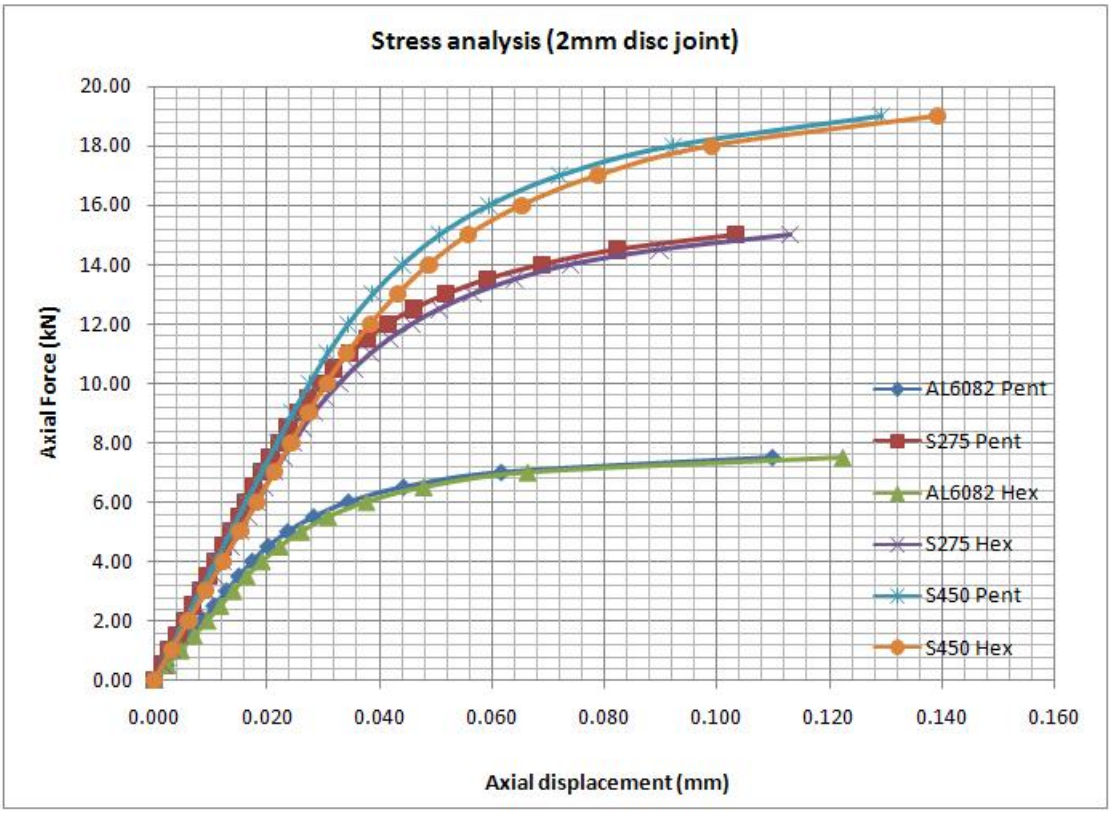

Figure 33: Stress analysis force-displacement plot for 2.0mm disc

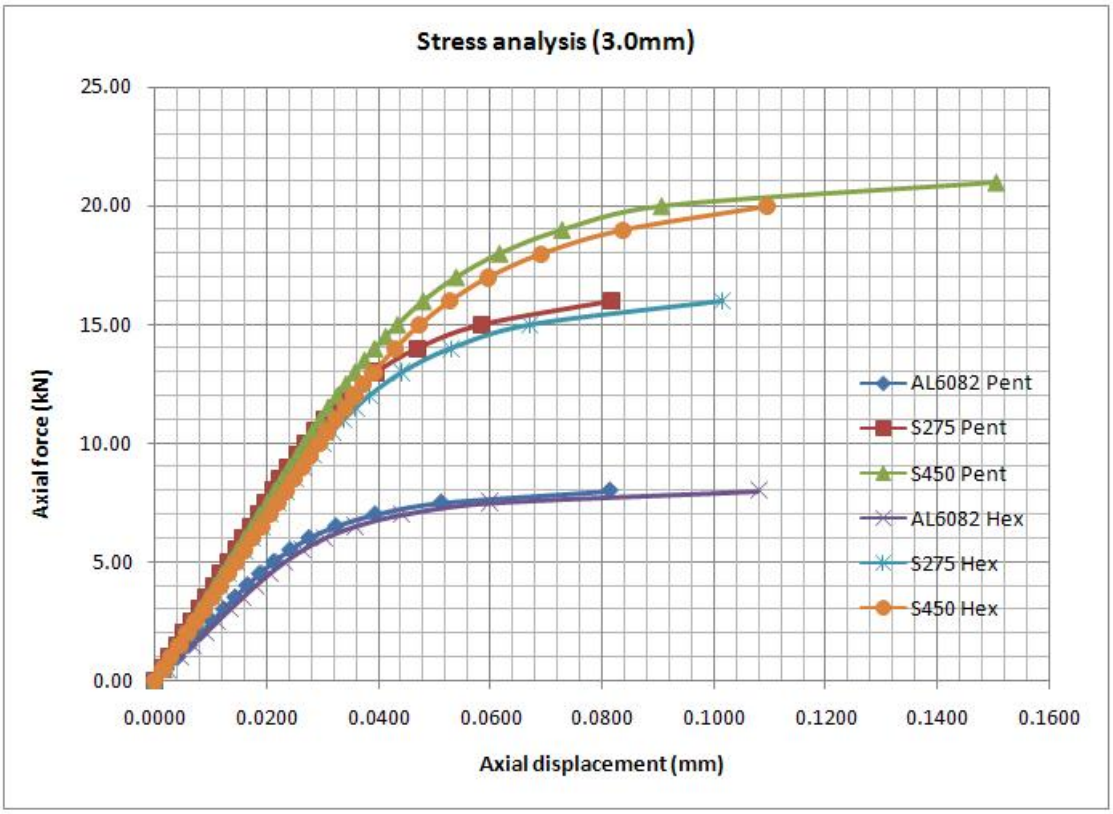

Figure 34: Stress analysis force-displacement plot for 3.0mm disc

Wind Loading

The following calculations determine the basic windspeed velocity for a geodesic dome structure built in an area nearby to Pabal, India. The calculations are guidelines from the Indian Standards, IS875 (Part 3): 1987, Wind Loads for Buildings and Structures. The relevant clauses to each calculation are given, and any assumptions are stated throughout.

Basic wind speed (clause 5.2)

Basic wind speed is based on peak gust speed averaged over a short time interval of about 3 seconds and corresponds to 10m height above the mean ground level in an open terrain (Category 2).

From figure 1, the Indian windspeed map gives: V_b = 39.0 m/s

Design wind speed (clause 5.3)

Design wind speed modifies the basic wind speed to account for terrain effects and the actual height of the building under consideration:

$$V_z = V_b k_1 k_2 k_3 k_4$$

Where:

Vz = design wind speed at any height z in m/s,
k_1 = probability factor (risk coefficient) (see 5.3.1),
k_2 = terrain roughness and height factor (see 5.3.2),
k_3 = topography factor (see 5.3.3)
k_4 = importance factor for the cyclonic region (see 5.3.4).

NOTE: The wind speed may be taken as constant upto a height of 10 m. However, pressures for buildings less than 10m high may be reduced by 20% for stability and design of the framing.

Assuming a standard design life of 50 years,
k_1 = 1.0 (Table 1, clause 5.3.1)

Assume that Pabal dome is built in category 2 open terrain, with well scattered obstructions:
k_2 = 1.0 (Table 2, clause 5.3.1)

Assuming no hills, cliffs or enscarpments that channel the wind are nearby:
k_3 = 1.0 (clause 5.3.3)

Assuming the structure is of normal importance (non-industrial and not of post cyclonic importance, such as a cyclone shelter, community building or water tank):

k_4 = 1.0 (clause 5.3.4)

Appendix C

Marek Kubik (Durham Univeristy)
Structural Analysis of Geodesic Domes

hence, assuming the height of the structure does not exceed 10m:

V_z = 39.0 x 1.0 x 1.0 x 1.0 x 1.0 x 0.8 = 31.2 m/s

Design wind pressure (clause 5.4)

The wind pressure at any height above mean ground level is obtained by the following relationship between wind pressure and wind speed:

$$p_z = 0.6 V_z^2$$

Where:

p_z = wind pressure in N/m^2 at height z, and
V_z = design wind speed in m/s at height z.

hence,

p_z = 0.584 N/m^2

The design wind pressure pd can be obtained as,

$$p_d = k_d k_a k_c p_z$$

Where:
K_d = Wind directionality factor
K_a = Area averaging factor
K_c = Combination factor (see 6.2.3.13)

For circular or near–circular forms, such as the Pabal dome, the wind directionality factor is:
K_d = 1.0 (clause 5.4.1)

Pressure coefficients are a result of averaging the measured pressure values over a given area. As the area becomes larger, the correlation of measured values decrease and vice-versa. The decrease in pressures due to larger areas may be accounted for with a reduction factor. Assume that no reduction factor applies to Pabal dome for simplicty, otherwise design pressure will become dependant on geometry.

K_d = 1.0 (clause 5.4.1)

Combining factors for wind pressure contributed from two or more building surfaces can allow a reduction factor because wind pressures fluctuate greatly and do not occur simultaneously on all building surfaces. However, assuming wind action on the Pabal dome acts in only one direction (worst case):

K_c = 1.0 (Table 19, clause 6.2.3.14)

hence,

p_d = 1.0 x 1.0 x 1.0 x 0.584 = **0.584** N/m^2

DO NOT SCALE

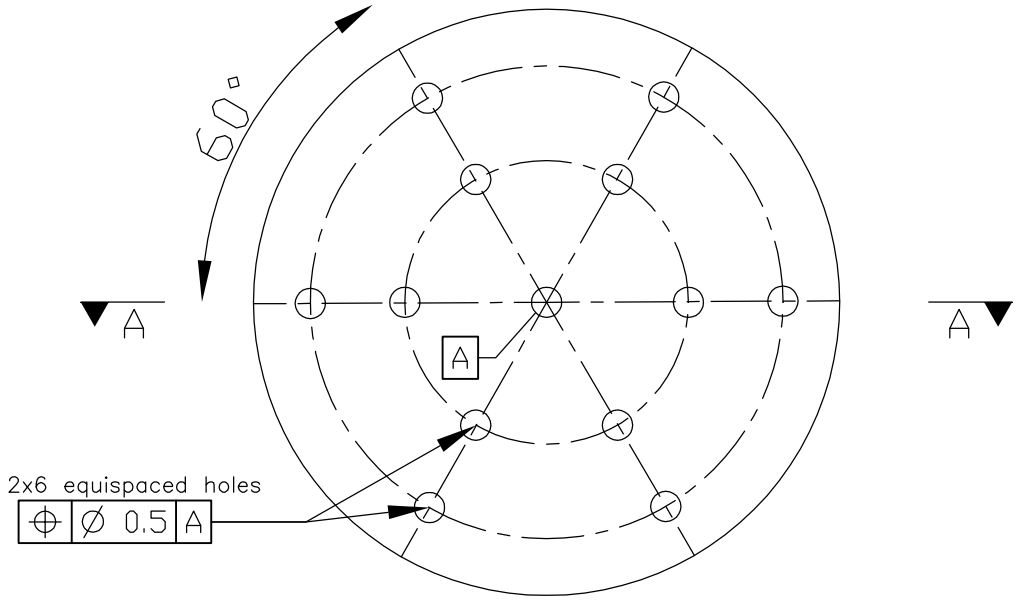

Hexagonal 'White' Disc
Elevation
1:2 @A3

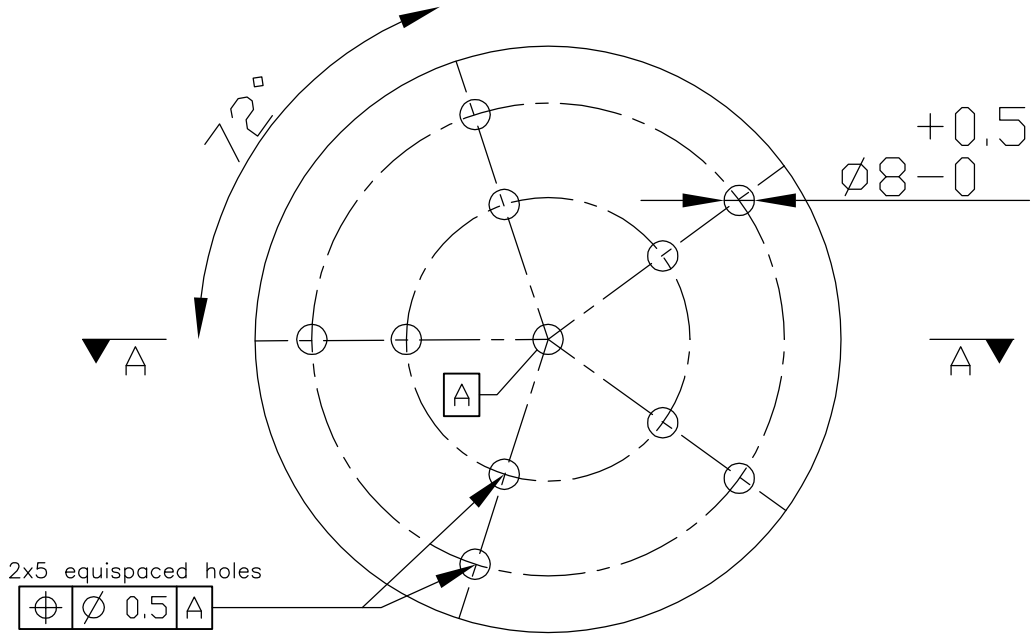

Pentagonal 'Black' Disc
Elevation
1:2 @A3

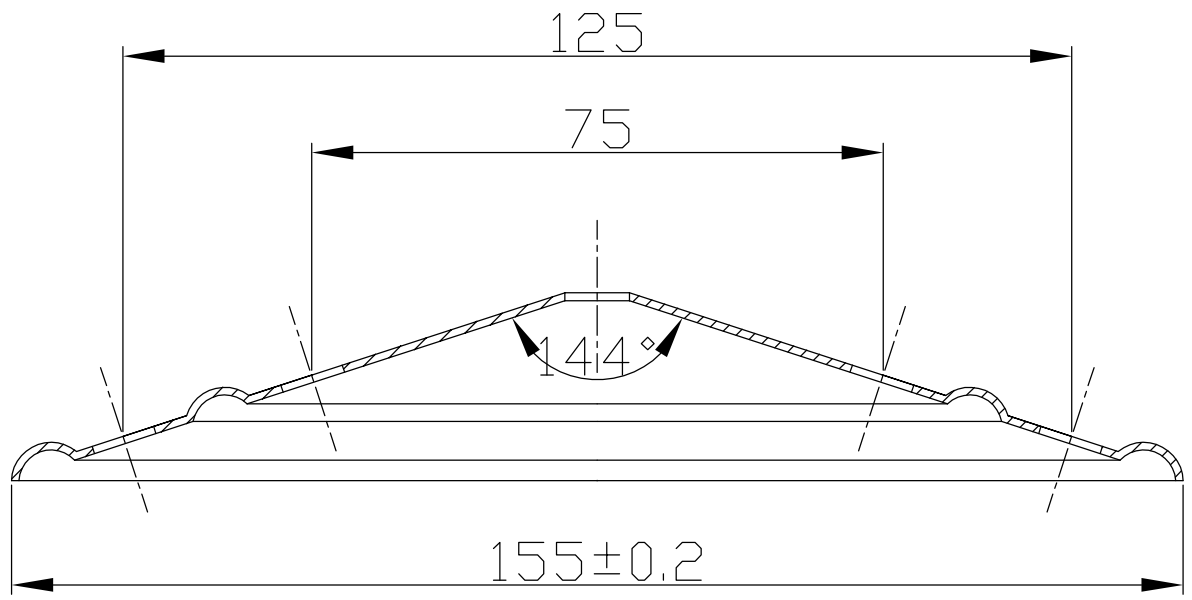

Section A–A
1:1 @A3

Notes

n1 All dimensions in mm.

n2 Crimp lines omitted from face views of discs for clarity.

n3 All drilled holes to be for nominal M8 bolts.

n4 Dimensions and tolorences apply to both elevations unless alternatively specified.

n5 Crimping to be achieved using a crimping ring fly press or similar.

n6 Section A–A describes the Pentagonal 'Black' Disc, but RHS bolt holes do not exist at section cut plane.

Durham University

School of Engineering

Project: Structural analysis of geodesic domes

Title: Hub joint technical details

Original Scale	Drawn	Checked	Authorised
1:2 @A3	M. Kubik		
	Date 10/11/08	Date	Date

Drawing Number: J001

Rev: –

1. Introduction

The following document provides fabrication details for the Pabal Dome designed by Vigyan Ashram, based on calculations that provide numerical proof of adequacy of the connection details. The structure was analysed using a Finite Element Analysis package, the most significant parameters and results of which are summarised below. The connection design, where possible, follows Eurocode 3, with all formulae and tables referenced where this is the case.

Contents

2. Dome Geometry

Dome type	V3 5/8ths	
Dome radius	3	m
Expand base to radius?	yes	

3. Forces applied

Self Weight

The following forces contributed to the self weight of the structure. These components include all the truss elements, joints and the weight of cladding:

Cladding density	22	kN/m^3
Cladding thickness	0.05	m
Elem section type	25x25x3	
Young's Modulus E	2.00E+11	N/m^2
Elem unit weight	77.2	kN/m^3
Joint weight	1	kg per joint
Coarse mesh	1.15	kg/m^2
Fine mesh	0.93	kg/m^2

Vigyan Ashram		Project No.	Sheet No.
Marek Kubik (Durham University) Pabal Dome Fabrication Details	Date. Feb 2009	09-001	002
Project.	**Appendix E - Example Calculations**	By. MK / Checked.	

Imposed and Wind Loading

Wind loading refers to the total force acting on a given face that was considered in the design, as determined by the wind loading code IS875 (Part 3). Imposed loading is an allowance for non-permanent forces (such as worker access for cleaning or painting).

Imposed load	0.6	kN/m^2
Wind force	7.22	kN

Soil Loading

Soil loading indicates whether the dome was analysed under conditions of partial or full burial under some type of soil:

Soil type	Black Cotton	
Soil depth	3.59	m
Angle buried	180	deg

Load Combination Factors

Load combination factors allow the user to weight the aforementioned loads before they are combined to form a combination load case that is used in the FEA analysis (factors of zero indicate the type of load was ignored).

Load	PSF
Self Weight	1.35
Soil	0.00
Wind	1.05
Imposed	0.75

4. Summary of FEA analysis

The following section provides a summary of some of the key results determined by the FEA solver:

Lagest positive displacement:	0.78	mm	@	DOF	451
Largest negative displacement:	-1.51	mm	@	DOF	13
Largest tensile force:	7.7	kN	@	beam	164
Largest compressive force:	-6.0	kN	@	beam	131

5. Calculations

The following design checks are made in these calculations:

1. Capacity of dome joint against shearing failure.
2. Capacity of bolted connection against shear and bearing failure.
3. Capacity of equal angle channel section used as member.
4. Deflections are not excessive under Servicability Limit State (SLS).

It is assumed that the critical case for design will always be tensile in the structure (i.e. any force that can be withstood in tension will also pass any compression checks), so the modulus of the greatest force as determined by the FEA Solver is taken as the ultimate design load:

$F_{v,Ed}$ = 7.7 kN

Design Assumptions

1. Joints are constructed from isotropic mild steel.
2. Bolt diameters, bolt holes and spacings used are homogenous (the same) throughout the structure.
3. The disc diameter is 77.5mm; **extreme caution** is required altering this radius significantly, as the joint capacity relationship was designed with this as a fixed parameter.
4. Members are sufficiently squat not to fail in buckling, and bending moments in the structure are negligible.
5. Bolts are assumed category A: Bearing type, in accordance to EC3 and are designed to withstand predominantly shearing action (due to axial loading).

Disc joint parameters

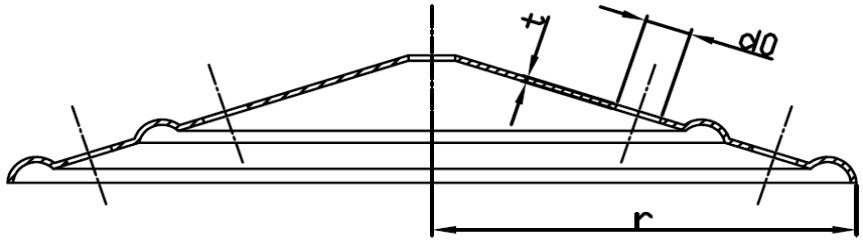

Disc thickness t	2	mm
Steel type	S275	
Bolt class	4.6	
Bolt diameter d0	10	mm
No. Bolts per connection	2	
Controlled bolt size	no	

Bolt spacings

The array of bolt spacings must conform to the spacing limits shown below on both the disc and the beam. If this is not possible with the number of bolts chosen, then either a higher grade of bolt class should be chosen or larger connecting members are required.

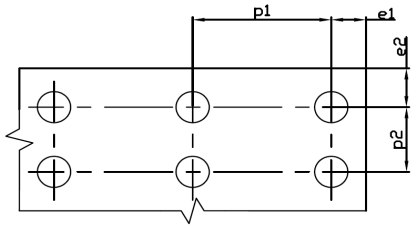

Spacing of bolt holes for members

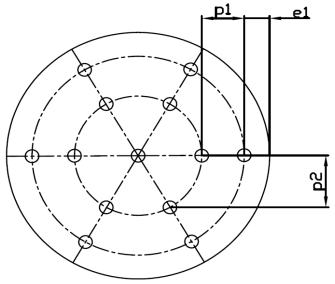

Spacing of bolt holes for disc

e_1	12.5	mm
e_2	12.5	mm
p_1	25	mm
p_2	25	mm

Limits:

12 ≤ e_1

12 ≤ e_2

22 ≤ p_1 ≥ 140

24 ≤ p_2 ≥ 140

Joint Capacity

The following joint capacity relationship was developed empirically following physical tension tests and Stress Analysis of the hub joints at the University of Durham:

$$F_{v,Rd} = \frac{f_u(4.13t + 26.43)}{\gamma}$$

Where:

t = 2 mm

f_u = 430 N/mm^2

γ = 1.05 (a safety factor on the load)

Check that disc joint capacity surpasses the ultimate design load:

$F_{v,Rd}$ = 14.2 kN > 7.7 kN **OK**

Appendix E - Example Calculations

Bolt Capacity

Two inequalities must be satisfied for safe design of bolts:

$F_{v,Ed} \le F_{v,Rd}$ (Ultimate load is less than design shear resistance - EC3 clause 3.6)

$F_{v,Ed} \le F_{b,Rd}$ (Ultimate load is less than desin bearing resistance - EC3 clauses 3.6 and 3.7)

Shear resistance capacity per shear plane:

$$F_{v,Rd} = \frac{\alpha_v f_{ub} A}{\gamma_{m2}}$$ (EC3 - Table 3.4)

Where:

A = 50 mm^2
α_v = 0.6
f_{ub} = 400 N/mm^2
γ_{m2} = 1.5 (a safety factor from EC3-67 Section 2)

$F_{v,Rd}$ = 8.0 kN/bolt

Bearing resistance capacity:

$$F_{b,Rd} = \frac{k_1 \alpha_b f_u d t}{\gamma_{m2}}$$ (EC3 - Table 3.4)

Where:

d = 10 mm
t = 2 mm
f_u = 430 N/mm^2
γ_{m2} = 1.5

α_b = MIN {

$\alpha_d = \frac{e_1}{3d_0} = \frac{12.5}{3 \text{ x } 10} = 0.417$ (Assuming that α_d is calculated for an end bolt, which is the worst case)

$\frac{f_{ub}}{f_u} = \frac{400}{430} = 0.930$

1.000

}

Hence:

α_b = 0.417

Water Bank Project Calculations

k_1 = MIN {

$2.8\frac{e_2}{d_0} - 1.7 = 2.8 \frac{12.5}{10} - 1.7 = 1.800$

2.500

}

Hence:

k_1 = 1.800

$F_{b,Rd}$ = 4.3 kN/bolt

To determine total design resistance of a connection provided by an array of bolts:

If $F_{v,Rd} \ge F_{b,Rd}$ then: $F_{Rd} = F_{b,Rd} \times n$

If $F_{v,Rd} < F_{b,Rd}$ then: $F_{Rd} = \min(F_{v,Rd}) \times n$

(where n is the number of bolts per connection)

Check that total design resistance of bolts are sufficient:

F_{Rd} = 8.6 kN > 7.7 kN **OK**

Angle Section Capacity

The final check Ultimate Limit State check is that the equal angle sections that make up the truss members will have sufficient resistance to the axial forces in the structure. The weakest point of these members is through the drilled section, and several equations exist for determining the section capacity, depending on the number of holes.

Chosen section size and other required calculation parameters:

Angle section:	25x25x3	
Steel grade:	S275	
f_u	430	N/mm^2
Cross Sectional Area A	157	mm^2
Net area at bolthole A_{net}	127	mm^2
Section thickness t	3	mm
β_2	0.4	
β_3	0.5	

$$N_{u,Rd} = \frac{2.0(e_2 - 0.5d_0)f_u}{\gamma_{m2}} = \frac{2.0 \times (12.5 - 0.5 \times 10) \times 3 \times 430}{1.5 \times 1000} = 12.9 \text{ kN} \quad \text{(1 bolt)}$$

$$N_{u,Rd} = \frac{\beta_2 A_{net} f_u}{\gamma_{m2}} = \frac{0.4 \times 127 \times 430}{1.5 \times 1000} = 14.6 \text{ kN} \quad \text{(2 bolts)}$$

$$N_{u,Rd} = \frac{\beta_3 A_{net} f_u}{\gamma_{m2}} = \frac{0.5 \times 127 \times 430}{1.5 \times 1000} = 18.2 \text{ kN} \quad \text{(3+ bolts)}$$

Check the angle capacity is sufficient:

F_{Rd} = 14.6 kN > 7.7 kN **OK**

Deflection Limit Check

The deflection limit check is a final check to ensure the size of deflections in the structure under the loading conditions assumed will not be excessive enough to lead to cracking or visual distortions. If this check fails, but the three Ultimate Limit State checks have been passed, then the structure is still structurally sound.

Are all member deflections within the limit (L/360)? **OK** (EC3 7.2.1)

6. Fabrication data

Member	Length (m)	No. Required
A	1.063	30
B	1.230	55
C	1.257	80
D	0.000	0
E	0.000	0
F	0.000	0
G	0.000	0
H	0.000	0
I	0.000	0
4 way connection joints		15
5 way connection joints		6
6 way connection joints		40

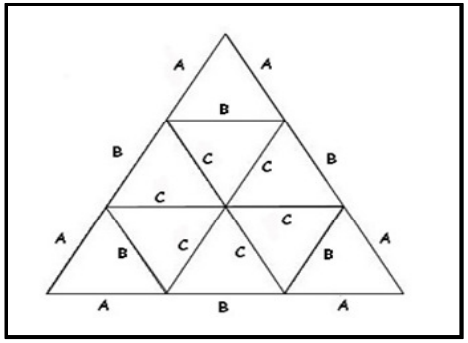

Assembly diagram of truss elements

7. Appendix

This appendix tabulates the values that have been looked up for calculations in various parts of the spreadsheet. It is not necessary to print this page.

Geodesic dome chord factors (unscaled)

	Member Length								
Dome type	A	B	C	D	E	F	G	H	I
V1	1.05146								
V2	0.61803	0.54653							
V3 3/8ths	0.34862	0.40355	0.41241						
V3 5/8ths	0.34862	0.40355	0.41241						
V4	0.25318	0.29524	0.29453	0.31287	0.32492	0.29859			
V5 3/8ths	0.198147	0.23179	0.225686	0.247243	0.255167	0.245086	0.261598	0.231598	0.245346
V5 5/8ths	0.198147	0.23179	0.225686	0.247243	0.255167	0.245086	0.261598	0.231598	0.245346
V6	0.162567	0.190477	0.181908	0.20282	0.187383	0.198013	0.205908	0.215354	0.216628

Geodesic dome fabrication data

	Required numbers											
Dome type	No. A	No. B	No. C	No. D	No. E	No. F	No. G	No. H	No. I	No. 4J	No. 5J	No. 6J
V1	25									6	5	0
V2	35	30								20	6	10
V3 3/8ths	30	40	50							15	6	25
V3 5/8ths	30	55	80							15	6	40
V4	30	30	60	70	30	30				20	6	65
V5 3/8ths	30	30	60	60	50	50	30	30	10	25	6	95
V5 5/8ths	30	30	60	60	50	50	30	30	10	25	6	120
V6	30	30	60	90	30	60	130	65	60	30	6	130

Table 3.1 from Eurocode 3 - bolt class nominal strengths

Bolt class	f_{yb} (N/mm^2)	f_{ub} (N/mm^2)
4.6	240	400
5.6	300	500
6.8	480	600
8.8	640	800
10.9	900	1000

EC3-31 nominal strength values for hot rolled structural steel

Steel Grade	f_y (N/mm^2)	f_u (N/mm^2)
S235	235	360
S275	275	430
S355	355	510
S450	450	550

Equal angle section data

Angle code	Area (mm^2)	Thickness (mm)
25x25x3	157	3
25x25x4	200	4
25x25x5	241	5
30x30x3	187	3
30x30x4	240	4
30x30x5	291	5
40x40x3	247	3
40x40x4	320	4
40x40x5	391	5
40x40x6	460	6